Electronic Thesis and Dissertation Repository

8-21-2020 6:00 PM

Simulation Approaches to X-ray C-Arm-based Interventions

Daniel R. Allen, *The University of Western Ontario*

Supervisor: Peters, Terry, *The University of Western Ontario*
Co-Supervisor: Chen, Elvis, *The University of Western Ontario*
A thesis submitted in partial fulfillment of the requirements for the Master of Science degree in Biomedical Engineering
© Daniel R. Allen 2020

Follow this and additional works at: https://ir.lib.uwo.ca/etd

Part of the Bioimaging and Biomedical Optics Commons, Graphics and Human Computer Interfaces Commons, and the Systems and Integrative Engineering Commons

Abstract

Mobile C-Arm systems have enabled interventional spine procedures, such as facet joint injections, to be performed minimally-invasively under X-ray or fluoroscopy guidance. The downside to these procedures is the radiation exposure the patient and medical staff are subject to, which can vary greatly depending on the procedure as well as the skill and experience of the team. Standard training methods for these procedures involve the use of a physical C-Arm with real X-rays training on either cadavers or via an apprenticeship-based program.

Many guidance systems have been proposed in the literature which aim to reduce the amount of radiation exposure intraoperatively by supplementing the X-ray images with digitally reconstructed radiographs (DRRs). These systems have shown promising results in the lab but have proven difficult to integrate into the clinical workflow due to costly equipment, safety protocols, and difficulties in maintaining patient registration. Another approach for reducing the amount of radiation exposure is by providing better hands-on training for C-Arm positioning through a pre-operative simulator. Such simulators have been proposed in the literature but still require access to a physical C-Arm or costly tracking equipment.

With the goal of providing hands-on, accessible training for C-Arm positioning tasks, we have developed a miniature 3D-printed C-Arm simulator using accelerometer-based tracking. The system is comprised of a software application to interface with the accelerometers and provide a real-time DRR display based on the position of the C-Arm source. We conducted a user study, consisting of control and experimental groups, to evaluate the efficacy of the system as a training tool. The experimental group achieved significantly lower procedure time and higher positioning accuracy than the control group. The system was evaluated positively for its use in medical education via a 5-pt likert scale questionnaire.

C-Arm positioning tasks are associated with a highly visual learning-based nature due to the spatial mapping required from 2D fluoroscopic image to 3D C-Arm and patient. Due to the limited physical interaction required, this task is well suited for training in Virtual Reality (VR), eliminating the need for a physical C-Arm. To this end, we extended the system presented in chapter 2 to an entirely virtual-based approach. We implemented the system as a 3DSlicer module and conducted a pilot study for preliminary evaluation. The reception was overall positive, with users expressing enthusiasm towards training in VR, but also highlighting limitations and potential areas of improvement of the system.

Keywords: C-Arm, Simulator, DRR, VR.

Lay Summary

Mobile X-ray imaging systems (C-Arms) are used in minimally-invasive procedures. Procedures such as facet joint or epidural steroid injections require the clinician to accurately guide the needle to the appropriate anatomical location. Because the clinician is unable to directly see the region they are directing the needle towards, they require X-ray imaging for guidance. Positioning the C-Arm accurately is a difficult task and can often induce excess radiation exposure to the clinician and patient. Extensive training for C-Arm positioning is critical for a successful procedure, but the current standard of training must be limited due to the harmful X-ray exposure to the trainee.

In order to provide a radiation-free solution for training, we have developed two C-Arm simulators. This first is a miniature 3D-printed C-Arm simulator which tracks the position of the X-ray source using cost-effective accelerometers and generates simulated X-ray images in real-time. The second is a Virtual Reality simulator using a scale C-Arm and the HTC Vive Pro for visualization. These simulators enable hands-on training for C-Arm procedures without exposure to ionizing radiation. We evaluated the miniature version via a user study consisting of medical residents. For the evaluation component, The users trained on our simulator performed significantly better than the control group. The VR simulator was evaluated positively for its use in medical education, however a followup study will need to be conducted for more conclusive results.

Acknowledgments

I would first off like to acknowledge my supervisors, Dr. Elvis Chen and Dr. Terry Peters. Elvis, thank you for being a great mentor, introducing me to this field through my capstone project, and pushing me to do a master's degree. Your patience and enthusiasm for teaching have made it easy to come to you with problems, and I have learned so much from you throughout the past 3 years. Terry, your leadership qualities create an atmosphere that make the VASST lab unique to so many other labs and I feel very fortunate to have ended up here. Thank you for all the fine-grained edits with my presentations and papers, they always pay off in the end and have made me a better researcher and communicator. I look forward to continue learning from you as I continue on to a PhD.

Thank you to John Moore, for your ingenuity in designing and building the miniature C-Arm. I appreciate you tutoring me through SpaceClaim, and discussions we have had on work and life advice in general. Thank you to my advisory committee, Dr. Collin Clarke, Dr. Narinder Paul, and Dr. Roy Eagleson for your support and guidance during my degree. Collin, thank you for providing the initial vision and continued support throughout these projects. I have enjoyed working with you these past few years and I hope we can collaborate together in the future. Thank you to Adam Rankin, for your vast knowledge of every piece of software and programming language used in the lab has truly been a saviour for me and everyone else, as has your efficiency as a lab manager in developing the software and hardware tools used in various projects. Your words of wisdom for presentations and posters has also been a huge help for me over these past two years.

Leah, thanks for being an awesome desk mate and always making time for my questions/distractions, IPCAI/France was such a great time and is definitely one of the highlights of my degree. Patrick, thank you for your endless help on coding problems and general discussions. I appreciate all of the good times in class, VR ping pong, TA'ing together, and our time in Houston of course.

Thank you to the rest of the VASST lab: Reid, Xiao, Wenyao, Lyla, Hareem, Shuwei, Joeanna, Robbie, Yingli, Goli and all of the other past members of the lab I have had the privilege of interacting with. I appreciate all the support and good times I have had with all of you at the grad club, lab parties, conferences and other events.

Last but not least, I would like to thank my family for supporting me through this endeavor. My brother Bryan Allen, thank you for all the great times growing up; the jam sessions, choreographed pool cue fights in the basement, and now for being someone who I can talk to about anything. Finally, thank you to my parents, Caron and Heath Allen, for raising me and supporting throughout my undergrad. You always believed in me even throughout the rough patches, and without that, I would not be where I am today.

Contents

List of Figures

List of Tables

List of Appendices

List of Abbreviations, Symbols, and Nomenclature

Terminology

2D	Two-dimensional
3D	Three-dimensional
4D	Four-dimensional
DoF	Degrees of Freedom
CPU	Central Processing Unit
GPU	Graphics Processing Unit
RAM	Random Access Memory
MC	Monte-Carlo
pose	Position and Orientation
IR	Infrared
LOS	Line of Sight
FOV	Field of View
RGBD	RGB + Depth
SLAM	Simultaneous Localization and Mapping
IMU	Inertial Measurement Unit
HMD	Head Mounted Display
TRE	Target Registration Error
VR	Virtual Reality
RMSE	Root Mean Squared Error
CAD	Computer Aided Design
GUI	Graphical User Interface

Medical Imaging Terminology

CT	Computed Tomography
US	Ultrasound
MRI	Magnetic Resonance Imaging
CBCT	Cone Beam Computed Tomography
FJI	Facet Joint Injection
XRII	X-ray Image Intensifier
ALARA	As Low As Reasonably Achievable
DRR	Digitally Reconstructed Radiograph
HU	Houndsfield Unit
OR	Operating Room
MRT	Medical Radiation Technologist

Chapter 1

Introduction

The aim of this thesis is to provide two approaches to facilitate the training of physicians and radiographic technicians for C-Arm manipulation during image-guided needle-based spinal procedures. Standard training employs an actual C-Arm using live X-ray exposure, which is both expensive and can subject the user to unnecessary radiation. The approaches proposed in this thesis reduce the need for training on a clinical machine, along with the accompanying radiation hazard.

This chapter provides the background and motivation behind the research outlined in this thesis. First, a brief overview of the anatomy of the spine and some of the common diseases and disorders are discussed. This is followed by the history of mobile fluoroscopic C-Arms and a description of the type of procedures that are the focus of this work, as well the training gaps and other issues associated with operation of the device. Lastly, a detailed review on the current solutions aiming to address these problems is presented, which formulate the motivation and research goals for this thesis.

1.1 Spinal Anatomy and Disorders

The spine can be broken down into three major sections: The Cervical, Thoracic, and Lumbar (see Fig. 1.1).

The spine not only serves as the foundation for how we are able to move our torsos but also as a housing and protection unit for the spinal cord. The disk ligaments (disks) between each vertebra act as shock-absorbers and protect the vertebrae from one another during movement. The facet joints enable the freedom of movement between each vertebra, detailed in Fig. 1.2

There are many tightly compact and high-risk structures surrounding the spine as highlighted in Fig. 1.3. The dural sac encases the spinal cord which is responsible for carrying out nerves to the entire body via the neural foramen. Damage to the spinal cord, neural foramen,

1
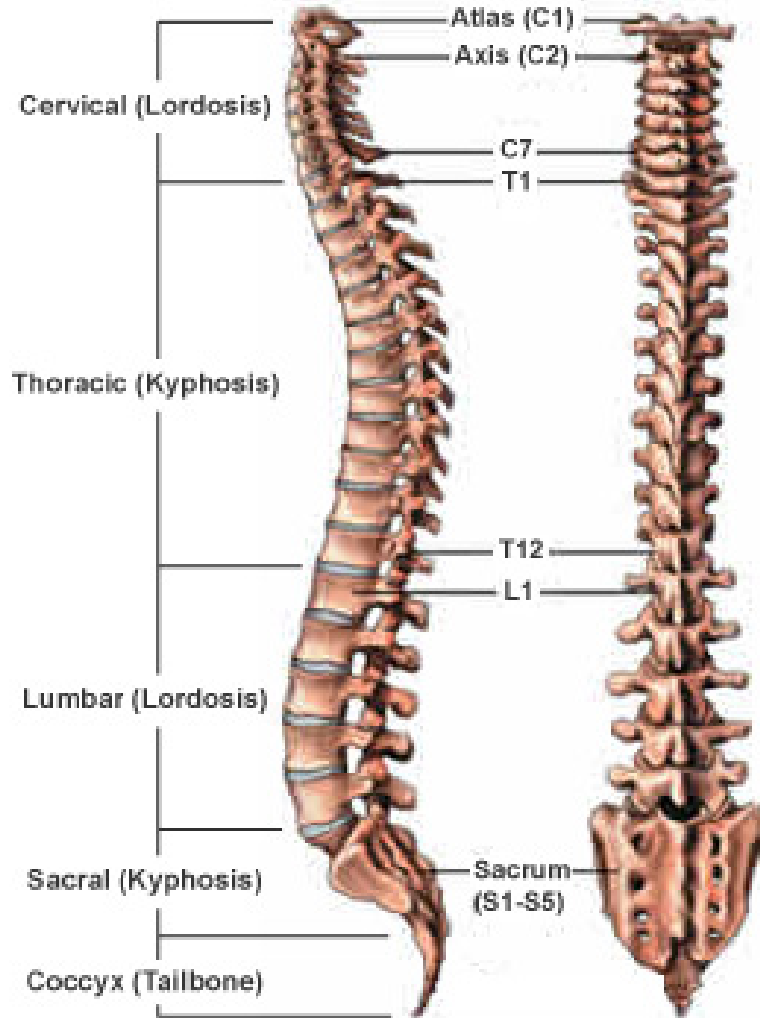
Figure 1.1: Medial-Lateral (left) and Anterior-Posterior (right) views of the regions of the spine (image courtesy of Nova Orthopedic and Spine Care).

and spinal nerves can cause severe harm including meningitis, paralysis, stroke, or death [17].

1.1.1 Herniated Disk

The disks in the spine consist of a soft inner layer (nucleus pulposus) and tougher outer layer (annulus fibrosis). A herniated disk occurs after significant mechanical stress causes the nucleus to push through a fissure in the annulus[1]. Due to the close proximity of spinal disks to the spinal cord and its nerve branches, the nucleus can cause inflammation and/or compression around a spinal nerve depending on the severity of the herniation (Fig. 1.4).

---

[1]https://www.mayoclinic.org/diseases-conditions/herniated-disk/symptoms-causes/syc-20354095
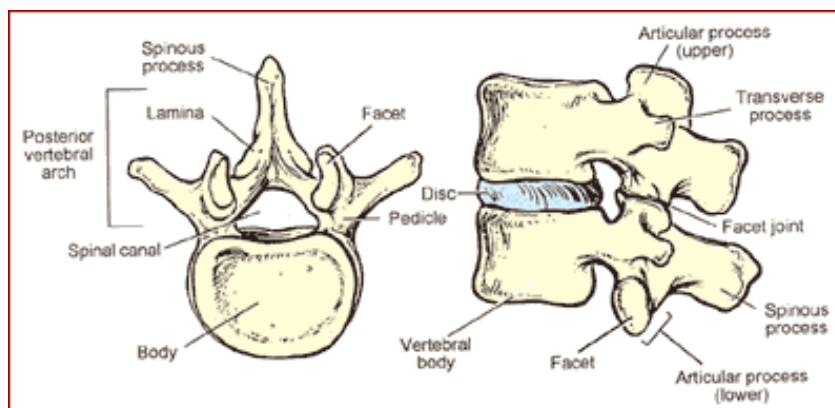
Figure 1.2: Superior (left) and Medial-Lateral (right) views of a vertebral body (image courtesy of USC Spine Center).
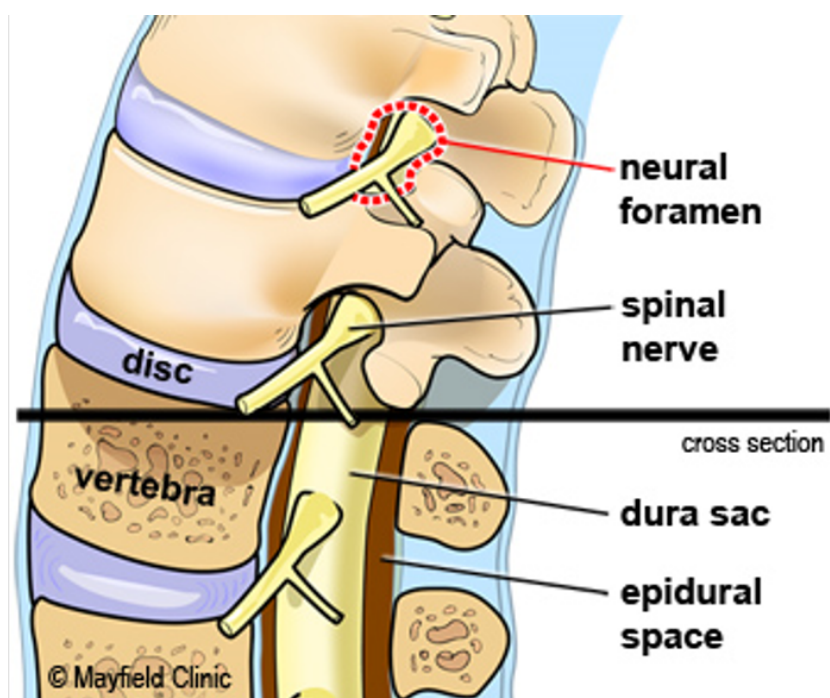
Figure 1.3: High-risk structures surrounding the spine (image courtesy of Mayfield Brain and Spine).

Herniated disks can often be treated with exercise and physiotherapy, however if the pain is severe they can be treated with epidural steroid injections. Section 1.4.2 gives an overview of this procedure.
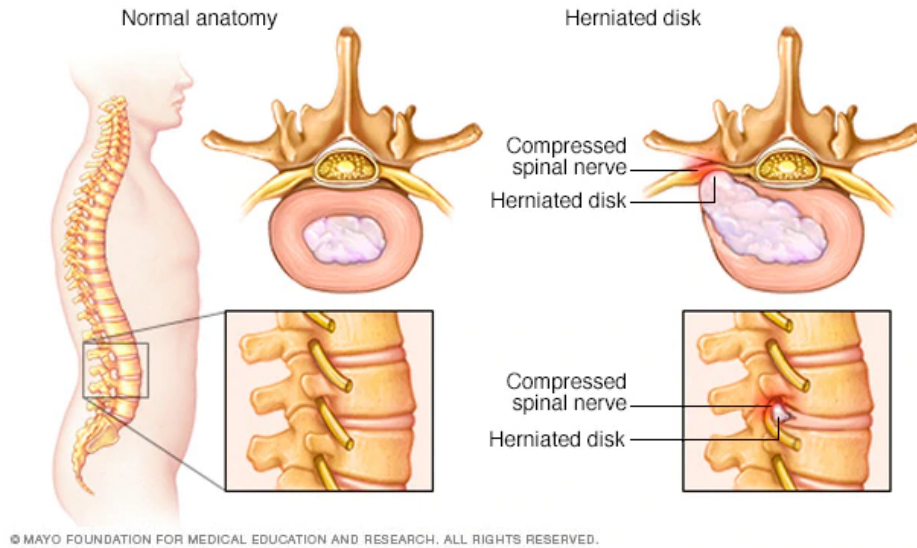
Figure 1.4: Normal disk structure compared to a herniated disk (image courtesy of Mayo Clinic.)

1.1.2 Facet Joint Syndrome

Facet Joint syndrome, like disk herniation, can occur after significant stress or movement of two adjacent vertebrae. It can also occur after years of wear and tear, where the cartilage between the vertebrae gets worn down over time. Similar to other forms of arthritis, this cartilage breakdown causes the joints to not move as freely and can cause inflammation around the area[2].
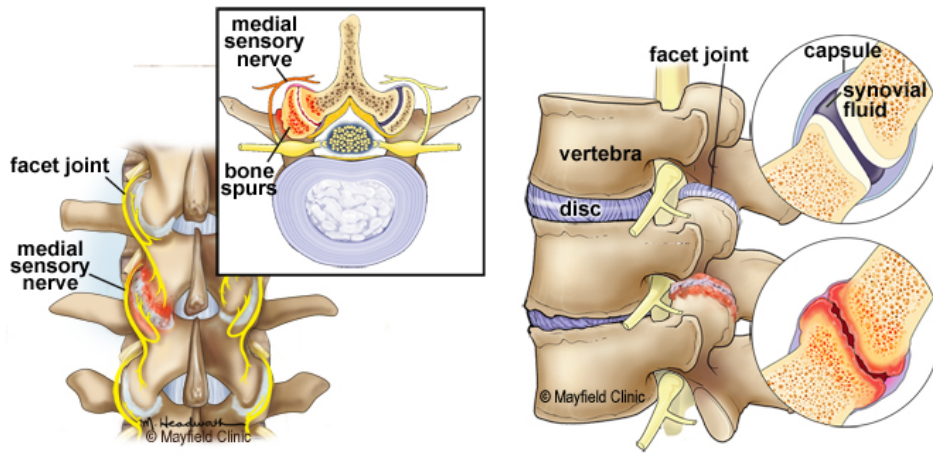
Figure 1.5: Facet Joint Syndrome is caused by inflamed cartilage around the facet joint putting pressure on the medial sensory nerve (image courtesy of Mayfield Brain and Spine).

---

[2]https://www.mayfieldclinic.com/pe-facet.htm

1.1.3 Diagnosis and Treatment

There is no universally accepted gold standard for the diagnosis of lower back pain [18]. Because of the closely packed nerve structures in the spine, symptoms of one disease can masquerade as the symptoms of another. An incorrect diagnosis not only leads to a failed treatment, but the wasted time and money puts a burden on the healthcare system.

Although X-ray fluoroscopy or radiographs can offer some information to help with a diagnosis, usually a complete 3D reconstruction of the patient is required in the form of Computed Tomography (CT) or Magnetic Resonance Imaging (MRI) scans. In conjunction with imaging, a complete physical exam and medical history of the patient is critical to gain a thorough understanding of the root cause of the pain[3]. This physical exam will typically involve joint manipulation and the performance of movement exercises which will help the clinician pinpoint the precise location of injury.

Depending on the age and physical ability of the patient, physical therapy is often the preferred initial treatment. However, sometimes the pain can be so debilitating that surgical intervention is required.

1.2 Imaging Modalities

With regards to interventional spine procedures, percutaneous approaches have replaced invasive methods due to the advancement of medical imaging, lower costs, shorter procedure time, and quicker patient recovery[4]. The imaging modalities used to facilitate these procedures are described in the next section.

CT, Ultrasound (US), and C-Arm fluoroscopy are examples of imaging modalities commonly used for these minimally invasive spinal procedures. The type and complexity of the procedure as well as institution-specific practice largely dictate the method that will produce the overall safest outcome for patient and clinician. This section summarizes the pros and cons for each imaging modality commonly used in lumbar spine procedures and why C-Arm fluoroscopy was chosen as the focus for this thesis.

1.2.1 CT

CT scans deliver a 3D (three-dimensional) reconstruction of the patient anatomy thus offering a higher degree of information than 2D (two-dimensional) US or fluoroscopy. This information can be visualized either through a set of 2D cross-sectional image slices (Fig. 1.6) or a 3D

---

[3]https://www.webmd.com/back-pain/back-pain-treatment
[4]https://www.beckersspine.com/spine/item/19204

volume rendering (Fig. 1.7). CT-guidance has seen success for procedures such as periradicular infiltration, percutaneous spinal disk decompression and facet joint blocks [20]. Unfortunately, the visualization benefits of CT come at a cost. Studies analyzing the correlation between CT radiation and increased cancer risk [27, 10, 44] have forced clinicians to scrutinize the risk/benefit ratio associated with using CT guidance intraoperatively. In particular, pediatric CT scans have been shown to significantly increase the lifetime radiation risk over adult CT scans [10].

Figure 1.6: Epidural steroid injection performed under CT guidance [55] (image courtesy of the American Journal of Neuroradiology).

Recent developments of CT scanners and integrated C-Arm Cone Beam Computed Tomography (CBCT) have enabled intraoperative CT guidance with much lower radiation dosages. C-Arm CBCT has also introduced the "single-suite" concept, reducing overall procedure time and radiation exposure by using the C-Arm for preoperative, intraoperative, and postoperative CBCT scans [56]. External guidance systems also reduce radiation exposure by limiting the need for repeated CT scans throughout the procedure, however as discussed in Sec. 1.6.4, integrating these systems into the clinical workflow is a difficult process. While extensive research has gone into making CT guidance safer, in many cases C-Arm fluoroscopy and US guidance techniques are capable of achieving the same procedure success [60, 61], and CT should only be considered for very complex or high-risk cases that require advanced visualization for a safe and successful procedure [37].

1.2.2   Ultrasound

Due to its low-cost, portability, and lack of radiation exposure, ultrasound has recently been explored as an alternative guidance method for percutaneous spine procedures such as nerve root blocks [30], lumbar punctures [45] and Facet Joint Injections (FJIs) [60, 61, 37]. In a
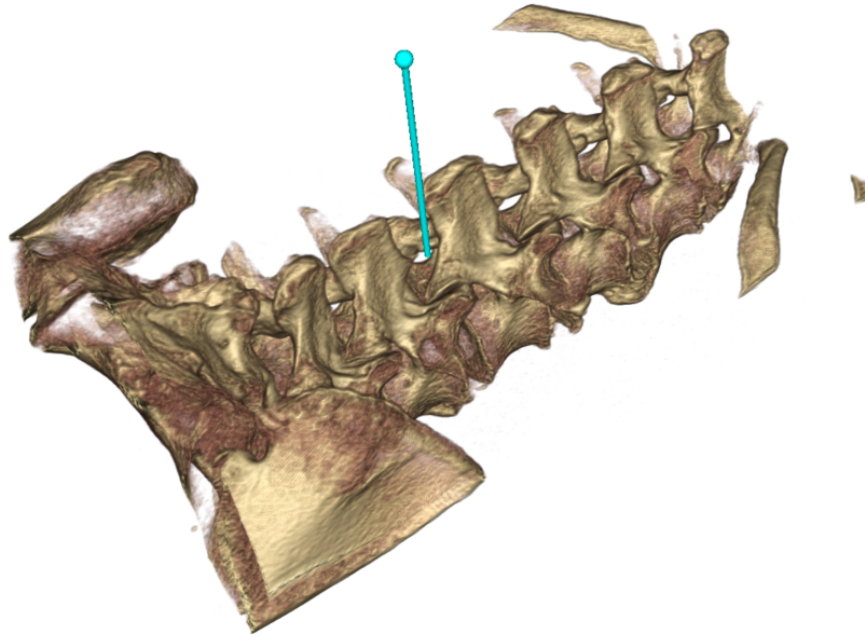
Figure 1.7: Needle model incorporated into a Spine CT volume rendering.

meta-analysis of controlled trials for US vs CT/flurosocopy-guided facet joint procedures, Wu *et al.* [60] showed that no significant differences in pain and functional improvement were noted between US and CT/fluoroscopy guided techniques in a total of 202 adults with facet joint pain. Ye *et al.* [61] showed no significant anatomical measurement differences between CT and US images and 86.5% of FJIs in the lumbar spine were correctly performed under US guidance.

Currently, there are many limitations in comparison to the other approaches to make US guidance feasible for widespread clinical acceptance. One of the most important of these limitations is the operator skill that is required to produce images with a high enough contrast between tissue to correctly identify the injection site [45]. The presence of additional fat tissue in obese or larger patients make this contrast even more difficult to acquire [37]. Furthermore, US-guided needle insertions are two-handed techniques that involve aligning the needle with the plane of the US beam at an appropriate trajectory. This is a non-trivial task and requires an additional level of skill and experience that many pain physicians will not have acquired. Fig. 1.8 shows the comparison of a US image to a CT image slice.
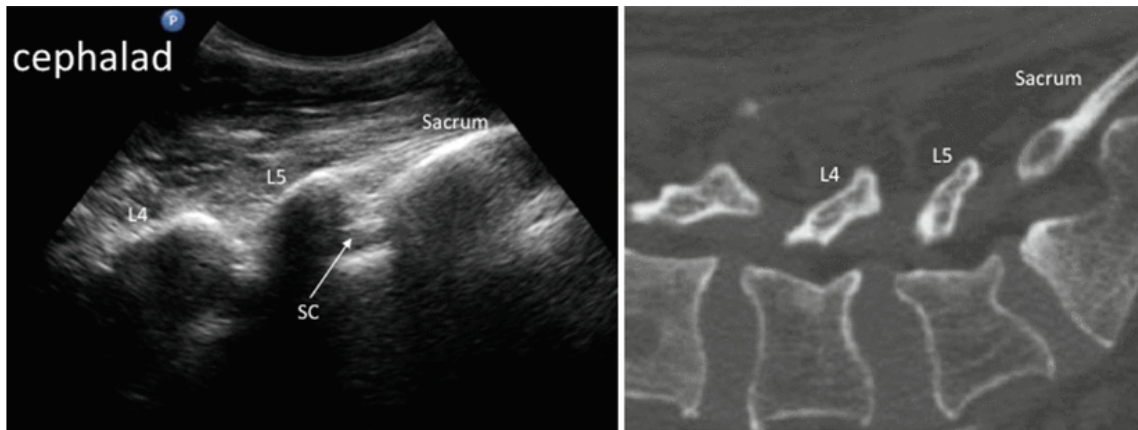
Figure 1.8: Ultrasound (left) vs CT (right) spine visualization (image courtesy of Anesthesia Key).

1.2.3 C-Arm Fluoroscopy

C-Arm fluoroscopy is the most commonly used image-guidance modality for percutaneous spinal interventions. Although C-Arm fluoroscopy does expose the patient to radiation, the levels are significantly lower than CT, especially with the advancement of lower-dose flat-panel C-Arms. Like US, fluoroscopy only offers a 2D image rather than a full 3D reconstruction. However, while US only offers a 2D slice of the patient in-plane with the US beam, fluoroscopy provides a 2D projection of the entire 3D anatomy thus facilitating a much higher level of visualization than a 2D US image (see Fig. 1.9[5]).

Many procedures, such as epidural steroid injections, lumbar punctures, and nerve root blocks, often require this higher level of visualization than US due to the relative high risk of the procedures. In fact, the relatively poor image resolution that US produces is considered a higher procedural risk than the radiation exposure induced by fluoroscopy [37].

Single fluoroscopic images usually present a low radiation exposure risk, but this risk can be significantly elevated when continuous (live) fluoroscopy is employed. A single second of live fluoroscopy, when compared to a single static fluoroscopic image, can produce up to 60 times the amount of exposure depending on the frame, or refresh rate of the C-Arm. Live fluoroscopy should be avoided whenever possible but is used in certain cases when a static image is not sufficient to accurately guide the needle. One common case where live fluoroscopy is used in spinal procedures is in verification of needle placement through contrast agent injection [20]. Often the clinician will need to see the dispersion of contrast agent in real-time in order to verify the correct needle placement. However, the need for live fluoroscopy is highly dependent on the skill and experience of the clinician [6].

---

[5]https://www.youtube.com/watch?v=4BG6LA9iS5Y

US and CT-guided techniques both offer their benefits in certain cases when compared to C-Arm fluoroscopy, and their use in spinal procedures are worth exploring as the technology continues to evolve. However, due to the overall benefits that C-Arm fluoroscopy provides, it is the standard clinical practice in local hospitals, and thus was chosen as the focus for this thesis.
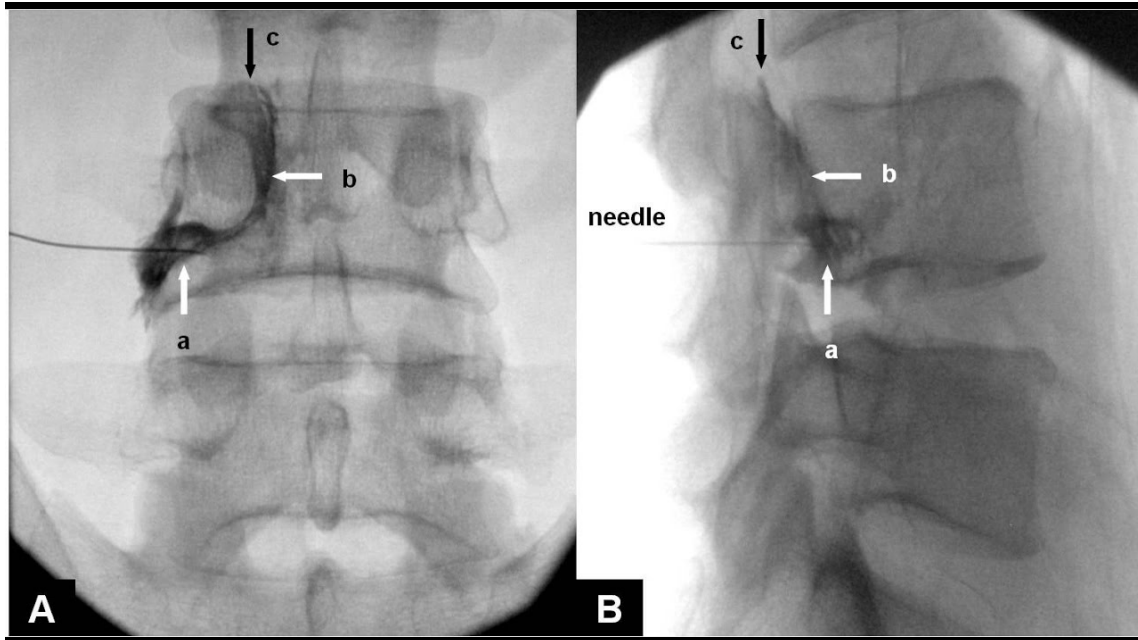
Figure 1.9: Anterior-Posterior (left) and Lateral (right) fluoroscopic view of the spine.

1.3 Mobile C-Arms

Mobile C-Arms are X-ray devices used intraoperatively for a variety of minimally invasive procedures. The "C" (gantry) comes from the C-like shape that connects to the X-ray generator to the detector (Fig. 1.10). The key innovation of the C-Arm over other X-ray devices is the ability to rotate about multiple degrees of freedom (DoFs). The kinematics of the C-Arm are described in more detail in section 1.3.2.

1.3.1 Background

The first C-Arm was developed by Philips in 1955, enabled by the development of the X-ray Image Intensifier (XRII) in 1951. Prior to this, X-ray images acquired on photographic film, could only be viewed after development of the film in a dark room, a process which took an average of 15 minutes [32]. XRII's are capable of real-time X-ray imaging and can produce

clear images with lower intensity X-rays, thus decreasing the radiation exposure to the patient and clinician. Image distortion is a consequence of XRII's due to the magnetic fields introduced by the prescence of ferrous objects in the viscinity of the XRII tube [43]. Modern C-Arms use flat-panel detectors, which limit the "pincussion" distortion around the edges of images seen with XRII's.

Figure 1.10: A Philips Zenition mobile C-Arm (image courtesy of Interventional News).

1.3.2   Kinematics

Most modern C-Arms operate with 6 Degrees of Freedom. For the remainder of this thesis the terminology illustrated in Fig. 1.11 will be used as follows: the lateral rotation describes rotation of the gantry about the longitudinal axis while the cranial/caudal tilt refers to the rotation about the frontal axis (cranial refers to rotation towards the patient's head while caudal refers to rotation towards the patient's tailbone). The "wag" rotation refers to rotation about the sagittal axis and can be achieved by pivoting the entire C-Arm on its wheels. Often this axis of rotation is offset from the C-Arm isocenter. The three translational DoFs can be achieved by movement of the entire C-Arm or the table. The device itself is typically moved rather than the

table as to not disrupt the patient, however some C-Arms do not provide elevation of the gantry component therefore requiring the table to be elevated in order to achieve translation about the sagittal axis.
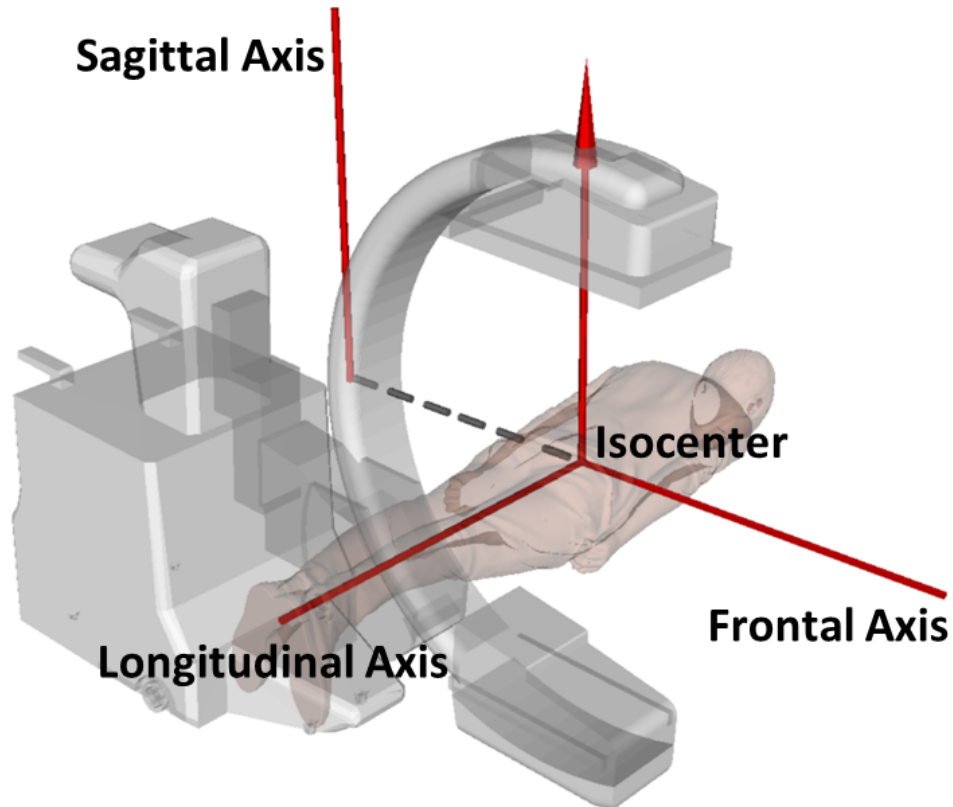
Figure 1.11: C-Arm axes of rotation.

1.4   C-Arm Fluoroscopy-Guided Spinal Procedures

C-Arm fluoroscopy plays a pivotal role in many modern-day percutaneous procedures. This includes many cardiac procedures, which will be discussed briefly in Chapter 4, however the focus of the research in this thesis is on spinal procedures for pain management. Facet joint and epidural steroid injections is the primary focus, however the research is directly translatable to other spinal needling procedures such as branch nerve blocks, transforaminal injections, and spinal radiofrequency ablation procedures.

1.4.1 Facet Joint Injections

A Facet Joint injection can be used to treat facet joint syndrome or arthritis. Typically a ~20° (varies depending on patient anatomy) lateral rotation is applied to the C-Arm in order to visualize the facet joint clearly in the X-ray image. This is typically called a "Scotty Dog" view due to the rough outline of a dog that can be seen for an optimal view (Fig. 1.12). To ensure optimal needle trajectory the needle should be seen as a dot in the image, known as a coaxial view. Contrast agent is sometimes injected in order to verify needle placement, followed by the slow injection of anesthetic and anti-inflammatory medication into or around the joint. Patients may feel pain relief for weeks or even years following the injection, however this range varies highly and some patients may require a more involved procedure if the pain does not abate too much[6].
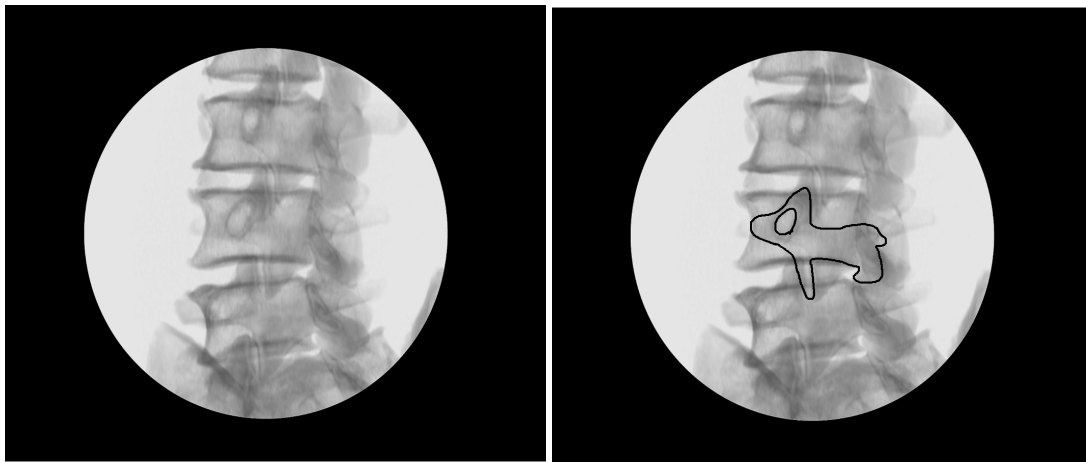
Figure 1.12: Scotty Dog view (Left) with dog outlined (right).

1.4.2 Epidural Steroid Injections

An epidural steroid injection involves the injection of medication into the epidural space rather than into the facet joint[7]. Fig. 1.3 shows the epidural space in which the clinician must insert the needle into for a successful injection. This injection requires extremely high accuracy as advancing the needle too far can pierce the dural sac or even the spinal cord. Damage to the spinal cord is a catastrophic risk involved in these procedures and can cause critical issues and even death in some cases [17].

---

[6]https://www.mayfieldclinic.com/pe-facet.htm
[7]https://mayfieldclinic.com/pe-esi.htm

1.4.3 As Low As Reasonably Achievable (ALARA) Principle

Due to the harmful effects of the ionizing radiation associated with X-ray, the As Low As Reasonably Achievable (ALARA) principle is generally followed for intraoperative X-ray use [47]. This means that the clinician should use the minimal x-ray exposure needed to achieve the task safely.

1.4.4 Procedure Difficulty

For many procedures, the correct manipulation of the C-Arm to achieve the desired X-ray image is a difficult task. It can be especially difficult if the patient has spine pathology and/or extra fat layers attenuating the X-ray path obscuring an otherwise "clean" image. In general, for needle injections, the clinicians are looking for the end plates to be "squared off", meaning the top and bottom end plate of the vertebral body should directly overlap in the image. A small deviation in C-Arm positioning can cause the optimal view to be compromised. Fig. 1.13 shows the change in image caused by an just an 8° caudal rotation of the C-Arm. The view of the end plates becomes obscured and is not sufficient for a safe needle insertion. Positioning the C-Arm optimally often requires several tries, referred to as "fluoro-hunting". Clinicians aim to reduce the amount of time spent fluoro-hunting so as to minimize the amount of radiation exposure to both the patient and the operator, and also the total procedure time.

1.5 Standard C-Arm Training and Gaps

The current standard of training for C-Arm guided spinal procedures involves apprenticeship-based programs and/or training on cadavers. Apprenticeship-based programs involving real procedures are very useful for showing the trainee the correct way to position the C-Arm and/or perform the needle insertion, however it is unethical for the trainer to demonstrate the incorrect way to perform the procedure or potential mistakes that could be made. This is a very limiting factor as understanding the potential mistakes and wrong approaches are the often the best way to enforce good practice. Cadaver-based training serves as a means to free up the hands-on demonstration and practice with needle insertions, however the complimentary task of positioning the C-Arm and shooting X-rays to guide the insertion must be limited due to the ALARA principle. Furthermore, if the trainee has only prior theoretical knowledge and no hands-on C-Arm training, much of this valuable training time could be spent just understanding the nature of the C-Arm kinematics. Because of these reasons, it is highly desirable to have some prior hands-on experience with a C-Arm simulator along with the complimentary

(a)   (b)

(c)
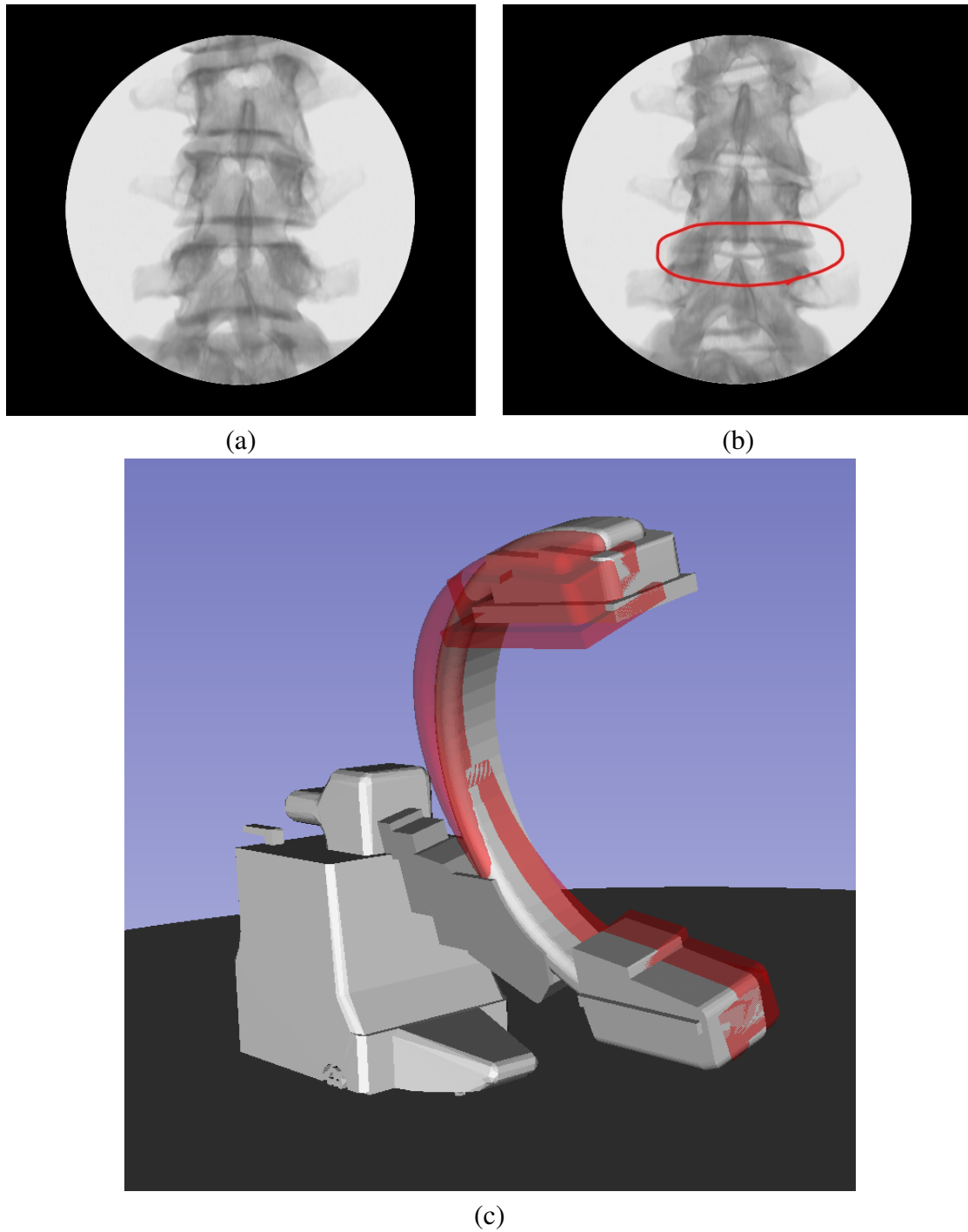
Figure 1.13:   A perfect full AP (a) vs an imperfect full AP view (b). The non-overlapping end plates are circled in red in (b). The difference in C-arm angles (c). The semi-transparent red gantry is rotated 8 degrees further in the caudal direction than the opaque gantry.

theoretical knowledge. The research for this thesis was motivated by an unmet need within the anaesthesia and interventional radiology communities for a simple training device.

1.6 Existing Solutions

In general, two main approaches have been taken when it comes to addressing some of the limitations associated with C-Arm positioning in interventional radiology. The first comprises solutions that fall under the category of intraoperative guidance systems. These systems aim to reduce radiation exposure directly by augmenting the intraoperative workflow. The second comprises approaches that indirectly affect the amount of radiation exposure in the OR by providing better training to clinicians using pre-operative simulators. The core technology for both of these approaches is the Digitally Reconstructed Radiograph (DRR).

1.6.1 Digitally Reconstructed Radiographs

DRR's are simulated X-ray images usually derived from a pre-operative CT using volume rendering techniques. Fig. 1.14 illustrates the underlying principle. Vectors (representing the direction of virtual X-rays) are traced from a point source (virtual X-ray source) through the voxels of the volume to each pixel on a 2D plane (virtual screen) behind the volume. The intensity value at each pixel is a result of the summation of attenuation that each ray received along its path.

https://www.researchgate.net/
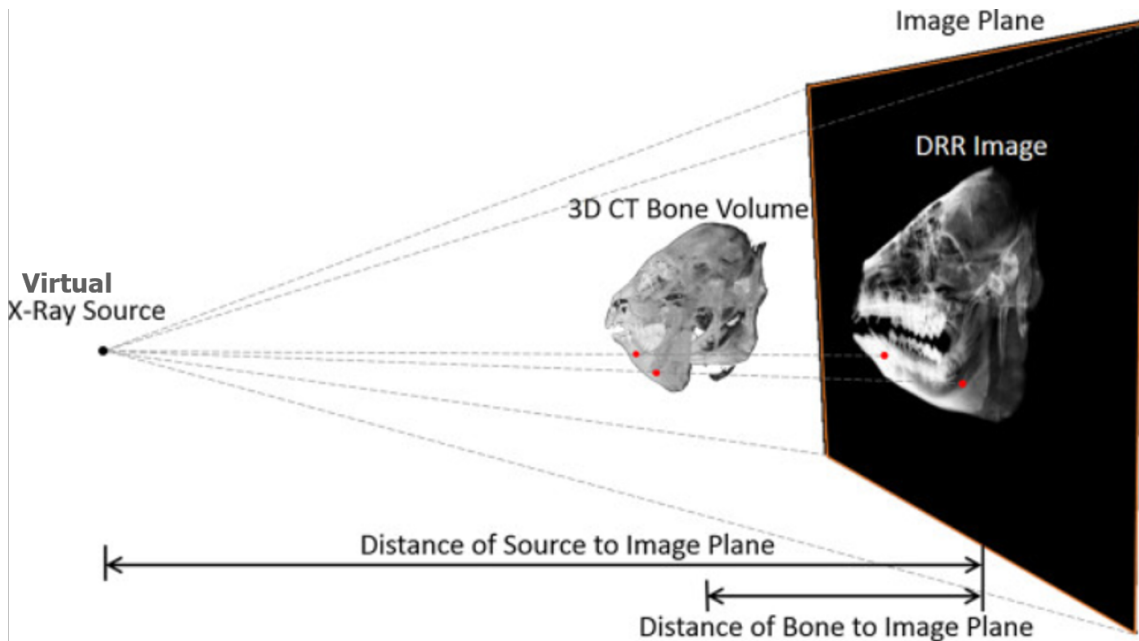
Figure 1.14: Visual depiction of how a DRR is generated from a CT volume [34] (image courtesy of Springer Nature).

There are number of different volume rendering approaches for DRR generation such as ray-tracing [39], splatting [4], shear-warp [11], and deep learning-based approaches [52, 51, 3]. Ray-tracing, compared to splatting and shear-warp is much more computationally expensive but able to produce higher quality images. The reason for the high computational load in ray-tracing techniques is due to the calculations required for each pixel in the desired projection. For every pixel, a ray is cast through the 3D virtual scene, and the resulting pixel value is calculated with respect to the encounters that ray received along its path. For highly realistic renderings, this computation is further burdened by additional calculations required from intersections with light rays, and secondary rays produced from transparent or reflective objects. With a Central Processing Unit (CPU) renderer and limited Random Access Memory (RAM), a realistic rendering consisting of several objects could take up to several minutes to produce a single frame, depending on the complexity of the scene.

Ray tracing is commonly used in volume-rendering and surface mesh rendering techniques. Volume rendering requires the ray to pass through the entire volume, recording the value (Hounsfield Unit(HU) value in the case of a CT volume) of each voxel it encounters, and factoring this into the calculation for the final pixel value. Surface rendering only involves factoring in the intersections of the ray as it enters and exits the object. For a fully opaque model, the only calculation required is the angle of incidence between the ray and the first front-facing polygon it encounters [42]. In the context of DRR generation, surface rendering can be used but generally produces less realistic results than volume rendering (see Fig. 1.15). Depending on the application, surface mesh rendering could be preferred due to the decrease in computation time and the fact that surface models are considerably smaller than volumes in terms of data storage.

Monte Carlo (MC)-based DRR generation methods [33, 2] outperform traditional ray-tracing methods in terms of image quality by simulating the probability of scatter each voxel could exhibit on every virtual photon. Ray-tracing is inherently procedural and thus not able to natively simulate statistical processes such as X-ray scatter or noise. The result is "high-exposure" images that simulate what an X-ray image would look like assuming no scattering of the primary beam and zero noise. For realistic scatter estimation, an appropriate number of photons must be simulated, which is typically on the order of 10^{10} for a single X-ray image. As a consequence, the generation time for a single DRR using MC simulation scatter estimation can be on the order of hours [2]. There have been proposals in acceleration strategies if prior knowledge of the problem exists, however, even reducing this generation time down to minutes would not be acceptable for the purposes of training or intraoperative guidance.

Machine learning-based approaches have been explored for DRR generation extensively in recent years, due to their ability to outperform traditional methods in diagnostic radiology.
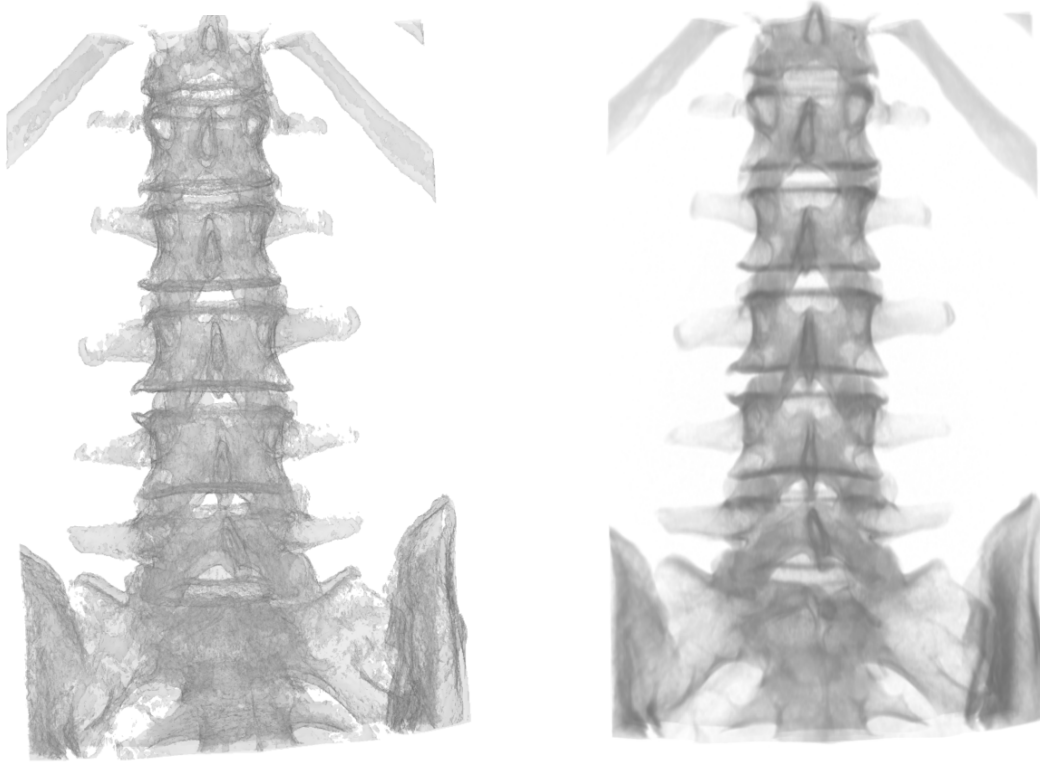
Figure 1.15: Spine DRR rendering of a surface model (left) and CT volume (right).

One of the limiting factors to developing machine learning-based DRR generation methods is the lack of annotated intraoperative X-ray images available for training. The DeepDRR [52] network overcomes this bottleneck by training on realistic DRRs generated from CT datasets. The DRRs are generated through a machine learning pipeline of material decomposition, MC-based scatter estimation, and a poisson-gaussian noise injection model. The result is a network that, when trained on these DRRs, is able to generalize to previously unseen real X-ray images and detect anatomical landmarks [3]. DeepDRR was used recently to train a network aiming to automatically determine C-Arm position and orientation (pose) adjustments required to reach a standard projection view [31]. The results from this study are promising as they indicate that a neural network can aid the clinician in determining the correct C-Arm position, eliminating the need for excess fluoro-hunting. While a very promising tool for intraoperative fluoroscopy, DeepDRR is not necessarily suitable for use in a training simulator as the trained network still takes ~2.0 seconds to generate a single DRR.

The area of computer graphics in the past decade has been revolutionized by the introduction of dedicated graphic cards and stronger computing power. Graphics cards or Graphics Processing Units (GPUs) allow the rendering process to be sped up significantly by offloading the rendering parameters to a dedicated chip and freeing up the CPU for other tasks. Pixel val-

ues are computed in parallel and depending on the power of the GPU, number of cores, scene complexity, and desired image resolution, the image can be rendered with an adequately high frame rate (> 60 frames/second) for real-time visualization.

DRR Generation Algorithm	Advantages	Disadvantages
Splatting	Computation time	Image quality
Shear-warp	Computation time	Image quality
Ray-tracing	Computation time (GPU-accelerated)/Image quality	No scatter/ noise simulation
Monte-carlo	Scatter/noise simulation	Computation time
Deep learning	Scatter/noise simulation	Computation time

Table 1.1: Summary of advantages and disadvantages of common DRR generation algorithms.

Table 1.1 summarizes the advantages and disadvantages of the described DRR generation algorithms. We chose a ray-tracing approach for the projects in this thesis due to the highly realistic volume renderings that can be achieved in real-time. Choosing to simulate scatter via MC simulations or other methods would produce more realistic X-ray images, but suffer in computational speed. For the purposes of our applications, the training benefits of seeing the image update in real-time with respect to the C-Arm source outweigh the benefits of more realistic X-ray images with simulated scatter and noise.

1.6.2   Tracking Modalities

Generating a spatially accurate DRR requires precise tracking of the C-Arm source and detector with respect to the patient. Because the C-Arm gantry is a rigid structure when in motion, the source and detector remain fixed with respect to each other and the pose of one can be derived from the other. The systems described in the next two sections use various tracking modalities, each offering its unique benefits and trade-offs.

Optical Tracking

Optical tracking involves illuminating reflective tracking markers that are rigidly attached to an object, with pulses of infrared (IR) light, and recording the positions of the reflections with multiple (usually two) cameras. The object's pose is tracked in space via triangulation (Fig. 1.16). Optical trackers are typically very accurate (< 1mm) [58] but tend to be expensive. Furthermore, they require line-of-sight (LOS) from the tracker to the markers which is often difficult to maintain during interventional procedures. The Field Of View (FOV) can be a limitation for tracking the C-Arm source if the gantry rotations are very large.

The object is lit using near IR light   Retro-reflective markers reflect back
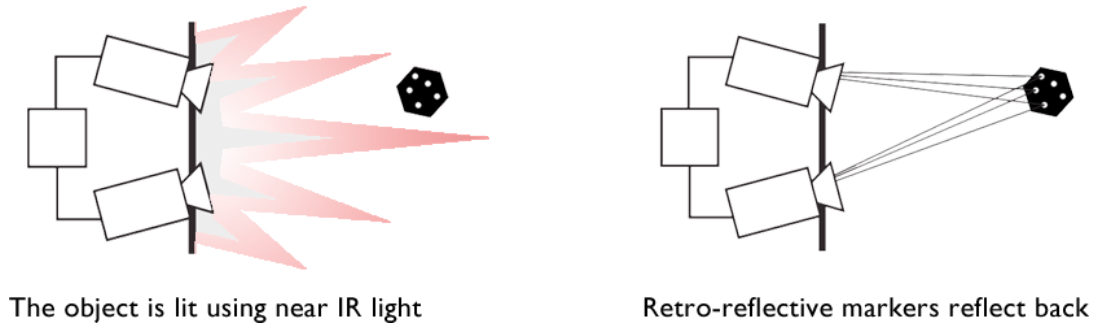
Figure 1.16: Object tracked in space via triangulation (image courtesy of ps-tech).

RGBD+Depth Cameras

RGB+Depth (RGBD) cameras also use IR sensors and triangulation for spatial tracking but employ an inside-out tracking approach [25] as opposed to the outside-in approach [40] used for optical tracking. RGBD cameras generate depth images from Time-of-flight IR sensors. Simultaneous Localization and Mapping (SLAM) algorithms are commonly used to track the camera's pose in space with respect to the objects around it[8]. SLAM tracking is commonly used for inside-out HMDs, such as the Microsoft Hololens[9] (Fig 1.17), in which there have been recent research developments in C-Arm tracking and visualization [50, 25]. RGBD cameras have also been proposed for C-Arm pose estimation that involve rigidly attaching the camera to the C-Arm source or detector and tracking natural or artificial fiducials located on the patient [38, 19]. RGBD cameras are more cost-effective and portable than optical trackers, but suffer in accuracy and are sensitive to illumination and the geometry of various features.

Mechanical Encoders

Integrated C-Arm mechanical encoders enable interpolation of the C-Arm pose through concatenation of encoder angles with the fixed radius of the gantry, addressing the FOV and LOS limitations associated with optical tracking. However, as encoders only track the pose of the C-Arm with respect to its isocenter and not the patient, 2D-3D registration [14, 19] of the intraoperative fluoroscopy images to the preoperative patient CT is required.

Accelerometers

Accelerometers are capable of measuring acceleration in 3 dimensions. When static, the only force acting on the accelerometer is the force of gravity. Each dimension has a component of

---

[8]https://www.andreasjakl.com/basics-of-ar-slam-simultaneous-localization-and-mapping/
[9]https://www.microsoft.com/en-us/hololens

Figure 1.17: The Microsoft Hololens employs RGBD cameras for inside-out tracking (image courtesy of CleanPNG).

the overall gravitational force acting on it depending on its orientation. When parallel to the ground, the x and y acceleration will have a magnitude of 0 and the z acceleration equals 1g (Fig. 1.18). Using this principle, we can use acceleration as a means of angular recovery of a static object. This approach fails for tracking the orientation of dynamic objects, for which a gyroscope is required.

Gyroscopes

Gyroscopes (Fig. 1.19) use the principal of angular momentum to obtain the orientation of an object. The law of angular momentum ensures that a spinning disk will remain in its spin plane unless an external force is applied to it [41]. Suspending such a disk in a 3-axis gimbal allows 3 degrees of rotation to be measured by recording the displacement between the disk and the gimbals. The caveat to this is that rotation about the axis perpendicular to the spinning plane cannot be measured, a difficulty that can be overcome by adding a second gyroscope with its spin plane in a different orientation to the first. For example, a typical gyroscope setup for an aircraft would have one gyroscope with its spin axis parallel to the gravitational axis to measure the pitch and roll rotation, and a second with its spin axis oriented in a perpendicular direction to measure the yaw rotation. This gyroscope can be synced with a compass for initialization and drift compensation.
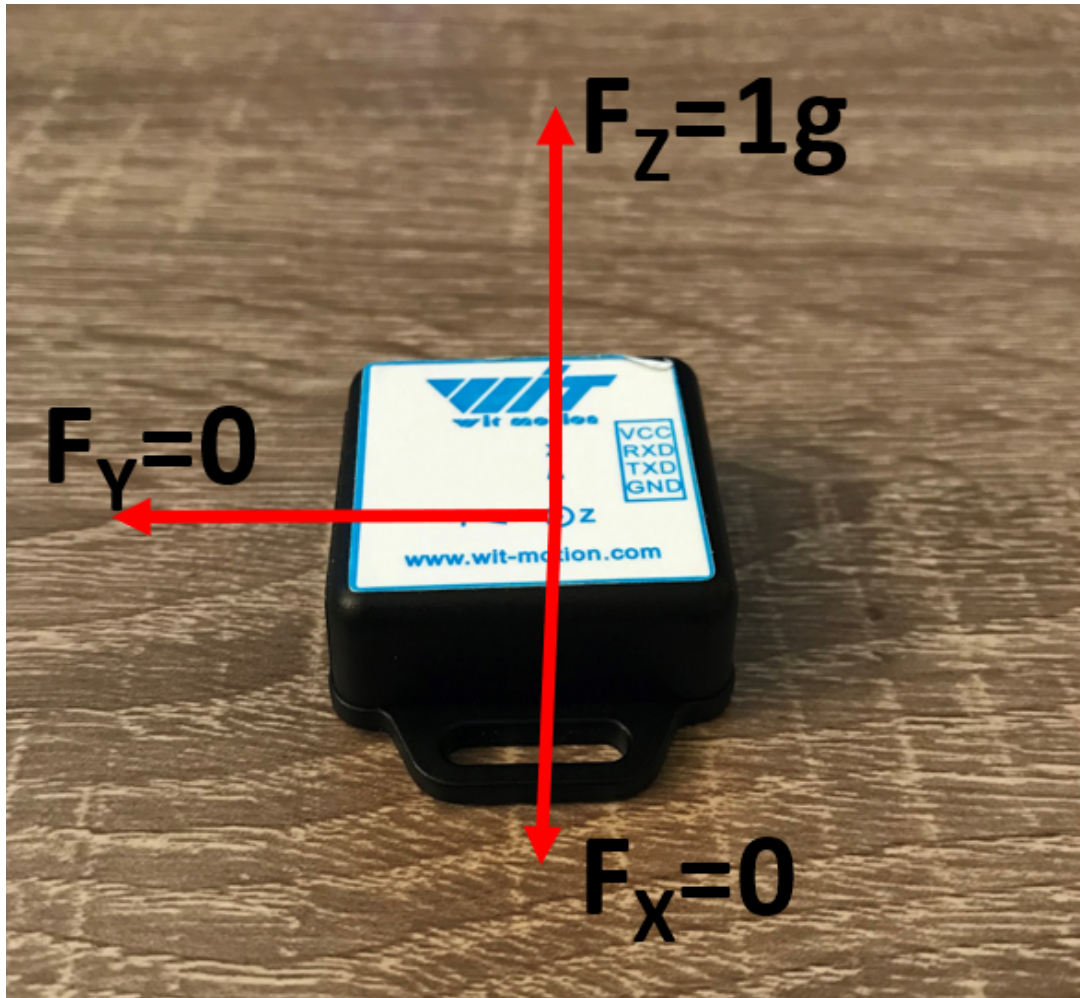
Figure 1.18: Forces acting on an accelerometer when level with the ground.

Inertial Measurement Units

Inertial Measurement Units (IMUs) contain sensors such as gyroscopes, accelerometers, and magnemometers to provide acceleration, angular velocity, and other forms of data useful for spatial tracking, and have been explored as a means of C-Arm pose recovery. Similar to mechanical encoders, IMUs do not suffer from LOS of FOV issues and can interpolate the pose of the C-Arm from the reported angles and the fixed radius of the gantry. However, they do not provide a means of tracking the patient and also require 2D-3D registration, or another technique for registering the patient to the pre-operative CT scan.

Figure 1.19: A 2-axis gimbal gyroscope (image courtesy of Educational Innovations).

1.6.3 Intraoperative C-Arm Augmentation

Although some of the systems described below demonstrate additional capabilities for training purposes, the primary motivation lies in augmenting the clinical workflow for intraoperative procedures.

C-Arm Positioning Using Virtual Fluoroscopy

De Silva *et al.* [14] propose a solution using mechanical encoders attached to the varying degrees of freedom of the C-Arm to recover its pose, which generate DRRs intraoperatively without the need for a costly tracking system. 2D-3D registration is used to rigidly register

the intraoperative 2D X-ray to the patient's pre-operative CT scan using a single X-ray image. They achieved a projection distance error of 1.6 mm when comparing the generated DRRs to the corresponding X-ray images. They conducted a pilot study in which 4 C-Arm operators were recruited to obtain optimal positions for 5 standard views in a pelvic trauma surgery using the conventional fluoro-hunting approach versus their proposed system. The operators were able to achieve more accurate angles, as well as reduce the number of X-ray images acquired down from 8 using the conventional approach, to 1 for the single X-ray image required for registration using the proposed system.

Camera Augmented Mobile C-Arm (CAMC)

The Camera Augmented Mobile C-Arm (CAMC) [38], developed at the Technische Universität München in Germany, offers a novel solution to C-Arm positioning difficulties. A webcam is fixed next to the C-Arm source on the side of the gantry and has its optical centre aligned with the X-ray source using a radio-transparent double mirror system. The webcam's image is calibrated to the X-ray image through a pattern consisting of spheres and torus' placed on the C-Arm's detector, enabling an augmented reality overlay of the X-ray image onto the video stream with a registration accuracy of < 1mm. The system was further developed to generate DRRs from a pre-operative CT scan by tracking the pose of the C-Arm via a planar marker pattern visible to the camera [15]. The DRRs were computed in real-time with the registration accuracy against the actual CT images varying from 1.1 to 4.1 mm. A separate study [57] evaluated the potential for the use of the CAMC to reduce radiation exposure for cadaveric intramedullary nail locking. They found that radiation exposure reduced by 28° when using CAMC vs a standard C-Arm.

Technician-in-the-loop C-Arm Repositioning

Underbath *et al.* [50] proposed the use of an optical see-through AR Head Mounted Display (HMD) for the purpose of C-Arm repositioning. They evaluated their system for the use in pelvic trauma surgery and were able to reduce the mean of 2.76 X-ray images normally required for realigning the C-Arm with a previous position down to zero. This system is very useful for procedures which require extensive repositioning of the C-Arm, however, it does not address the excess radiation exposure that occurs during "fluoro-hunting" for previously unacquired views.

Closing the Calibration Loop

Similar to the work mentioned above, the system proposed by Underbath *et al.* [25] uses an optical see-through HMD to aid in C-Arm positioning. The key advantage over previous approaches is the ability to provide visualization of pre and intra-operative 3D medical data directly at the surgical site by displaying it stereoscopically in the HMD. This greatly simplifies the complex spatial mapping of surgical tools and anatomy to 2D images that surgeons obtain through years of experience. The system utilizes SLAM-based tracking, eliminating the need for external outside-in tracking devices. The evaluated Target Registration Error (TRE) was 11.46 mm which could be improved with the advancement of the underlying SLAM tracking technology software and hardware.

Accelerometer Based Tracking

Grezda *et al.* [24] propose the concept of C-Arm pose recovery via accelerometers. They manufactured a miniature C-Arm mounted with a webcam and a calibration checkboard to provide the ground truth angles, and compared the accelerometer tilt-sensor readings to the ground truth angles to validate the use of the accelerometer for pose recovery. They found a sub-degree difference between the reported accelerometer readings and webcam angle readings, however the use of a webcam and calibration checkerboard is not necessarily a reliable measurement for the ground truth angles. This concept was expanded upon in [59], where they compared the use of an accelerometer for C-Arm tracking against two other methods: the built-in encoder and an image based technique using the tracking fiducial presented in [29, 28]. They used an optical tracker to obtain the ground truth angles and showed that the accelerometer achieved better accuracy than the other two methods with an angular error of 0.1 degree for both the primary and secondary rotational DoF's of the C-Arm.

1.6.4 Preoperative C-Arm Simulators

Integrating systems designed for augmenting or modifying the clinical workflow in interventional radiology can be a difficult task. While these systems appear to be useful and have proven to be effective for improving procedure performance in some studies, extending them to the domain of accepted clinical practice is met with significant roadblocks. This is often due to the rigorous clinical trials that must be performed, and safety measures that must be put in place, along with the willingness of clinicians to accept and learn different techniques for interventions.

Often the quicker and more ideal solution for improved patient outcome in the Operating Room (OR) can be achieved by providing better training through simulation approaches. Not

only has simulation-based training and education been shown to contribute to better patient care and safety [35], but in order to optimize the education that trainees receive, theoretical knowledge must be complimented by hands-on training [5].

This class of simulators describes systems designed primarily for the purpose of hands-on training for C-Arm procedures. The rigorous sanitary and ethical protocols which must be applied to intraoperative systems do not necessarily impact the design process, as these systems are not typically designed for use in the OR.

Some of the systems described below have the dual purpose of pre-operative training and augmenting the intraoperative workflow, although the primary motivation reported lies in the training aspect. A summary of the presented features for each described pre-operative simulator is presented in Table 1.2.

Simulator	Tracking Method	C-Arm	Evaluation Method
SimPORTAL	WebCam	Miniature model	Questionnaire
Mixed Reality C-Arm Simulator	Optical	Scale C-Arm	Questionnaire
AXIS	Optical	Scale C-Arm	Questionnaire/ Positioning Accuracy/ Radiation Exposure
IGSTK	WebCam	Fluoroscope	Questionnaire
VirtX	N/A	Virtual model	Questionnaire/ Procedure Time

Table 1.2: Summary of the methodology and evaluation for the reviewed pre-operative simulators.

3D Systems ANGIO Mentor

The 3D Systems (formerly Simbionix) ANGIO Mentor features a miniature C-Arm model which allows trainees to understand the basics of C-Arm fluoroscopy through manipulation on the miniature device. The module is geared towards angiography and highlights radiation safety training with regards to fluoroscopy time and C-Arm angulation.

SimPORTAL Fluoro-less C-Arm Trainer

The SimPORTAL Fluoro-Less C-Arm Trainer [54] developed at the University of Minnesota offers an example of a miniature C-Arm simulator designed for the purpose of percutaneous renal access training. They fixed a pair of webcams to the source and detector portion of a miniature C-Arm and combined this with a semi-transparent phantom to simulate X-ray images from the webcam videos. They were able to achieve highly realistic simulated X-ray images

and 92.8% of participants thought that the SimPORTAL system was of at least equal value to other existing Virtual Reality (VR) renal access training programs. However, the quality of simulated X-ray images is highly dependent on the quality of the semi-transparent phantom and would not be able to integrate new models quickly.

Mixed Reality C-Arm Simulator

Stefan *et al.* developed a C-Arm simulator [46] with the aim to complement and even replace large parts of cadaver training. From a patient CT scan, they 3D-printed a spine phantom which they then registered to the CT scan through a point-to-point landmark registration method. An outside-in optical tracker was used to track the pose of the C-Arm and phantom which was used to generate DRRs. They achieved highly realistic DRRs with a Root Mean Squared Error (RMSE) of 1.85 mm when compared to the corresponding real X-ray images. They conducted a user study which required 6 experts to perform facet joint injections and evaluate the system using a likert scale questionnaire. The results of the questionnaire showed strong agreement for the use of the system into medical education, however no quantitative feedback on user improvement (number of X-rays used, C-Arm placement accuracy, procedure time) after using the simulator was recorded. Although this is one of the few systems which incorporated tracked tools into the study, it was unclear whether or not they incorporated these into the DRRs.

Artificial X-ray Imaging System (AXIS)

Touchette implemented a physical simulator comprised of a clinical C-Arm and a mannequin [49]. The primary motivation for their system was to provide radiation-free C-Arm training for Medical Radiation Technologists (MRTs). The pose of the C-Arm is tracked using an optical tracking system and used to generate DRRs. In the context of pelvic trauma imaging, Touchette reported a 53 % decrease in scout image taken when aligning radiographic images and a 10 % increase in accuracy when the final images were taken. The DRRs were generated in 0.5 seconds, which while an improvement over previous approaches, still is not real-time and thus unable to simulate video X-ray or fluoroscopy.

Image-Guided Surgery Toolkit

A low-cost, high-fidelity fluoroscopy simulator is presented in [21]. This simulator generates DRRs from the registered pre-operative patient CT image volume, and the pose of the fluoroscope. They were able to achieve cost-effective tracking by using the Image-Guided Surgery Toolkit (IGSTK) [16] which has the capability of interfacing with cost-effective tracking devices. Gong *et al.* [21] mounted a webcam on a fluoroscope's intensifier and recovered the pose

of the X-ray source with respect to the patient, via a calibration phantom consisting of black-and-white planar marker patterns. By mounting the webcam on the fluoroscope's intensifier, they mitigated the LOS and FOV issues associated with an optical tracker. They conducted a user study using a 5-pt likert scale questionnaire, with clinicians reacting positively to the system. The key difference between this system and the others in this section is that they chose to simulate a diagnostic fluoroscope with only translational DoFs, thus not extendible to interventional C-Arm fluoroscopy.

VirtX Simulator

The VirtX simulator [7, 9, 8], developed at the Flensburg University of Applied Sciences in Germany, offers C-Arm training via a software application. Unlike the other training systems described in this section, VirtX does not offer hands-on training with a physical C-Arm but through a 3D computer model of a C-Arm rendered on a 2D display. The user interacts with the C-Arm through a keyboard and mouse, manipulating the various DoFs of the model, and is presented a real-time DRR generated from the position of the C-Arm X-ray source with respect to the virtual patient. The advantage of this system over others is the ability to perform the training in a non-medical environment, such as in the classroom or at home. The authors set out to isolate the benefits of training with VirtX by conducting a user study [7] in which they defined a C-Arm positioning evaluation task and divided the participants into three groups: 1) Training using VirtX only, 2) Training with VirtX followed by classic C-Arm training on a physical model, and 3) The control group training with a physical model only. Group 2 achieved a statistically significant lower procedure time than group 3. Group 1 also achieved a lower time than group 3 but the difference was not statistically significant. 91 % of all participants evaluated virtual radiography as helpful for understanding C-Arm operation and 83 % thought that VirtX was a useful addition to conventional C-Arm training.

The system was further developed to incorporate stereo visualization of the training environment through a HMD [48]. The motivation behind this extension is clear, as understanding C-Arm operation is a highly 3-dimensional task, and the "flattening" effect of the 3D computer model on a 2D screen with the classic VirtX program was a hinderance. Furthermore, the enhanced immersion of Virtual Reality has shown to help in knowledge retention [26]. 41 medical professionals were recruited to evaluate the system in which 39 fully agreed the system was relevant for medical education. The system was evaluated very positively in terms of lack of radiation, 3-dimensional spatial reasoning, and practice. One interesting feature of the system was the non-medical task of generating virtual radiographs of objects with a simple and known geometry, such as a stack of coins. Although demonstrating very promising results in terms of the overall user experience, no quantitative evaluation was performed in terms of re-

duction of radiation exposure, total procedure time, or C-Arm positioning error. Furthermore, the underlying technology of the system does not allow for seamless integration of tracked surgical tools into the environment to enable expansion into simulation for end-to-end medical procedures. This will be discussed in further detail in section 3.2.1.

1.7 Summary

Spinal disorders such as facet joint arthritis and herniated disk syndromes can cause such debilitating pain to the patient that it affects their daily quality of life. This pain can be managed quite effectively through minimally invasive procedures performed under C-Arm X-ray guidance. The downside to these procedures is the excess radiation exposure to which the patient and clinician are subjected to, which can vary greatly depending on the complexity of the procedure and skill of the clinician. Standard training techniques such as apprenticeship-based programs and cadaver training are limited due to the ALARA principle and access to OR time. To this end, many training simulators have been proposed in the literature which aim to reduce or eliminate the need for radiation entirely by generating DRRs. Most of these solutions rely on having access to a physical C-Arm which limit their accessibility.

1.8 Objective 1: Miniature C-Arm Simulator

The motivation behind the project presented in Chapter 2 was to develop a system which combined the benefits of training on a physical C-Arm as seen in [46, 49], while remaining cost-effective and accessible like the VirtX simulator presented in [7].

To this end, we have developed a miniature 3D printed C-Arm simulator using wireless accelerometer-based tracking primarily for the purpose of C-Arm training. The development and evaluation of the simulator are presented in chapter 2.

1.9 Objective 2: Virtual Reality C-Arm Simulator

The second objective of this thesis was to embrace the concept of C-Arm training with an entirely virtual C-Arm, but while maintaining the 3-dimensional visualization through the use of an HMD. The lack of haptic feedback can be justified by the fact that C-Arm manipulation is often achieved through communication from the clinician to the MRTs, who in turn manipulate the C-Arm as requested. Therefore, it is reasonable to hypothesize that visualization alone is sufficient to provide adequate C-Arm positioning training to the clinician.

The concept of C-Arm training through an entirely virtual means had been proposed by [48] and evaluated with very promising results. We build upon this concept by developing a custom VR C-Arm simulator on top of the 3DSlicer [10] (Slicer) [53] platform, with the aim of quantitative evaluation of C-Arm training for spinal procedures in VR. The development and evaluation of the simulator is presented in chapter 3.

---

[10]`https://www.slicer.org/`

Chapter 2

Miniature C-Arm Simulator Using Wireless Accelerometer Based Tracking

This chapter is largely based on the conference proceedings:

- "Miniature C-Arm Simulator Using Wireless Accelerometer Based Tracking" published in proceedings volume 11315: Medical Imaging 2020: Image-Guided Procedures, Robotics Interventions, and Modeling at the Society for Optics and Photonics (SPIE) 2020 conference [1].

2.1 Introduction

To Summarize Chapter 1, mobile X-ray C-Arms have enabled minimally-invasive procedures to be performed under X-ray guidance. Procedures such as epidural steroid injections can cause immense relief of chronic pain and significantly improve the quality of life for many patients. Improper placement of the needle can cause serious harm to the patient, such as paralysis, meningitis, stroke, or death. Therefore, finding the optimal X-ray image to best guide needle placement is a critical task in these procedures. Furthermore, because X-rays are a form of ionizing radiation, the ALARA principle is followed. Conventional training using real X-rays on cadavers or anthropomorphic phantoms is expensive and must be limited due to the ALARA principle.

Many systems have been proposed which aim to reduce (or eliminate entirely) the amount of radiation used in C-Arm procedures [14, 38, 24, 25]. However, the focus for most of these systems has been on generating DRRs intraoperatively to reduce the amount of fluoro-hunting required during the procedure. The use of expensive/bulky equipment, as well as patient-CT registration difficulties, render integration into the clinical workflow difficult for these systems.

Another approach to reducing the amount of radiation used intraoperatively is to provide more accessible, hands-on training to clinicians and MRTs. One such system which focuses on the training aspect is the VirtX C-Arm simulator proposed by Bott *et al.* [8]. This solution provides a virtual model of a C-Arm with which the user can interact using a computer interface. This provides an excellent means of accessible training but is still limited in the sense that the user is displayed only a "flattened" model of a C-Arm (on a 2D monitor) and cannot interact with it physically.

In order to address the limitations of previous approaches, we have developed a miniature 3D-printed C-Arm simulator that consists of a 10:1 scale C-Arm model, wireless accelerometers and a custom software application to generate real-time DRRs based on the accelerometer orientation data. It offers the benefits of training on a physical C-Arm while remaining cost-effective and portable. The WitMotion IMU[1] can track the primary and secondary rotations of a C-Arm head with a precision of $0.05°$, and provide the necessary tracking at low cost. An overview of the system is shown in fig 2.1.
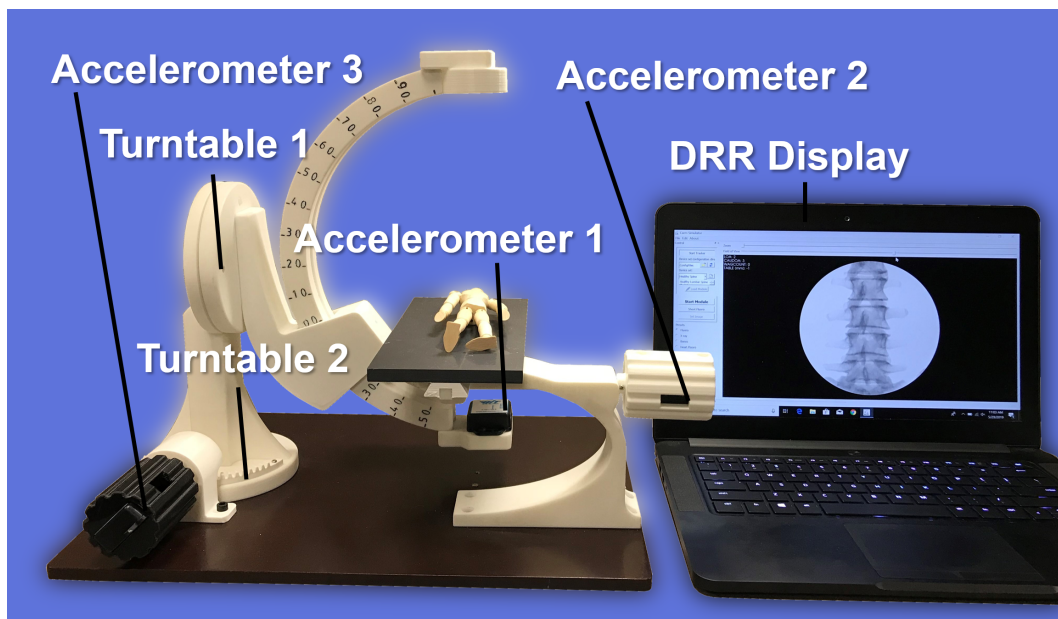
Figure 2.1: The proposed system. Accelerometer 1 used for the tracking of the lateral and cranial/caudal DoFs enabled by Turntable 1 and the rollers (hidden from view), accelerometer 2 used for tracking of the translational DoF of the table, accelerometer 3 used for the tracking of Turntable 2, real-time DRR display updated via serial port bluetooth connection.

2.2 Methods

The development of this system can be broken down into three main components: (i) the manufacturing of the C-Arm, (ii) the development of the software application, and (iii) integrating components (i) and (ii) together. This section first describes the C-Arm design, kinematics, and manufacturing process. This is followed by the DRR generation process, including the pose estimation calculation required for positioning the virtual camera. Next the software application is described, highlighting its features along with the architecture employed to tie the components together. Finally, the user design is presented, which attempts to validate the system as a training tool.

2.2.1 Assembly

The physical components were designed in Spaceclaim [2] and then 3D-printed using PLA plastic on an Ultimaker S5 3D printer[3]. The component breakdown is shown in Fig. 2.2. The support and holder sections are connected via a pair of parallel metal plates (turntables) which rotate freely about one another. The gantry is connected to the holder by a set of three ball bearings which clamp down on either side of the gantry (see Fig. 2.3).
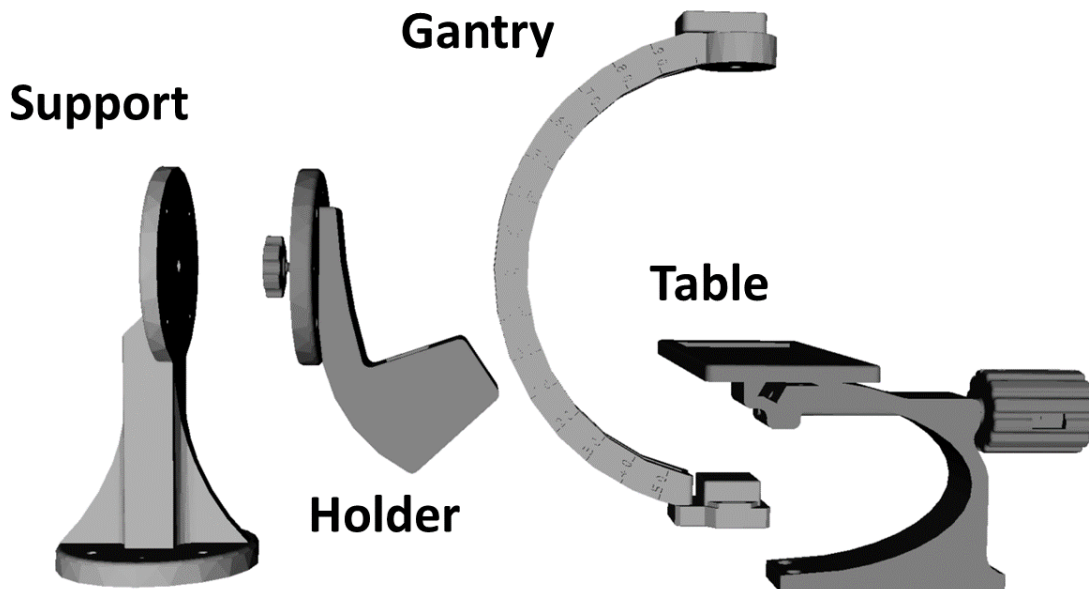
Figure 2.2: Breakdown of the physical components.

---

[2]http://www.spaceclaim.com/en/default.aspx
[3]https://ultimaker.com/3d-printers/ultimaker-s5
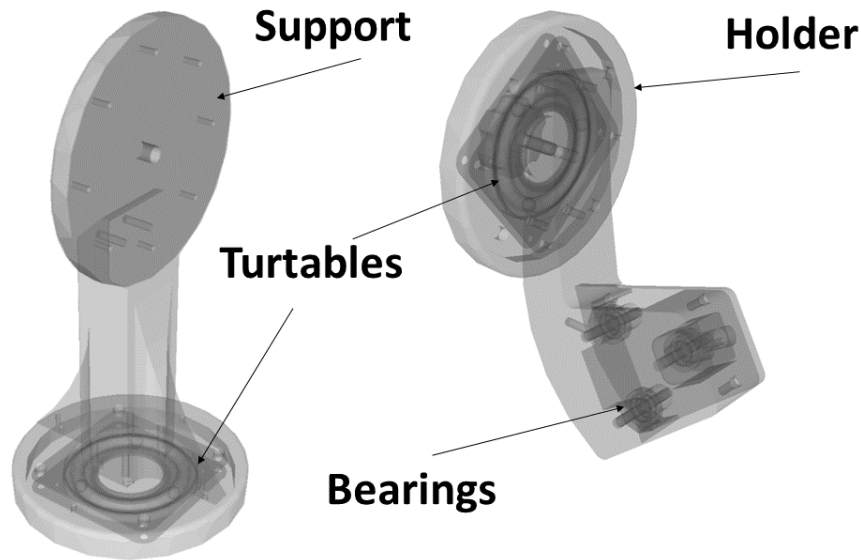
Figure 2.3: Semi-transparent support and holder models to show metal turntables and ball bearings enabling the rotational DoF's.

2.2.2 C-Arm Kinematics

To provide support for most fluoroscopy-guided spinal procedures, the C-Arm was designed to provide 4 DoF's: the primary rotation (lateral), secondary rotation (cranial), tertiary rotation (wag), and one translational DoF along the Y axis. Many straightforward spinal procedures only perform lateral and cranial rotation of the C-Arm, as well as translation of the table along the Y axis (Fig. 2.5) to navigate to the desired vertebra. The wag rotation is only performed in certain cases, but the choice to incorporate this DoF was made specifically for task of achieving a full lateral view on a patients with pathology. The remaining two translational DoFs are sometimes used in practice, but were not considered for this version as the additionally complexity required for tracking them would not have been worth it for the frequency these DoFs are used.

The lateral rotation is enabled by 3 ball-bearing rollers housed inside the gantry support component. The cranial rotation is provided by a mechanical turntable (turntable 1 in Fig. 2.1), and the wag rotation is provided by a second turntable (turntable 2 in Fig. 2.1). A semi-circular gear ring was fixed onto turntable 2 and interlocks with a smaller circular gear sitting vertically attached to the black handle in Fig. 2.1. Rotating this handle about the Y axis rotates turntable 2, and thus the entire C-Arm, about the Z axis. Similarly, for the translational DoF, a linear gear

is fixed to the bottom of the table and interlocks with a smaller circular gear fixed to a second handle via a cylindrical axle. The purpose of these gear mechanisms and rotating handles was to provide a user-friendly, intuitive means of manipulating the C-Arm, but more importantly, to enable a drift-free means of tracking the 3rd and 4th DoF using the IMUs.

2.2.3 C-Arm Tracking

As described in Sec. 1.6.2, IMUs contain a variety of sensors and are used to provide various measurements pertaining to the inertial motion of an object. Accelerometers provide acceleration information about an object, which while stationary, can provide an orientation from the effect of gravity on each axis. Gyroscopes recover orientation dynamically through the principle of angular momentum.

For tracking we used the 9-axis WitMotion JY901 Bluetooth IMU which contains a built-in accelerometer, mems gyroscope, and temperature sensor. The IMU has an output rate of 50 Hz over a serial port bluetooth connection, and a dynamic X and Y angle measurement of $0.05°$ accuracy. The dimensions are shown in 2.4. As there is no practical reference frame for tracking the Z rotation (axis parallel to gravity), we only used the X and Y rotation measurements reported from the gyroscope. We used these reported angles along with fixed values obtained from design to track the pose of the C-Arm source.

The first IMU was used to provide the angular data for the primary and secondary rotational DoFs of the C-Arm (see Fig. 2.4). The second IMU was housed inside the first rotating handle and employed for tracking the wag rotation while the third IMU was housed inside the second rotating handle and employed for tracking the table translation. The WitMotion IMU was added as a new device to the Plus Toolkit [4] to enable easy integration with Slicer for potential use in a broad range of applications.

Although we did not use the accelerometer data reported from the IMUs, for consistency, I will be frequently referring to the IMUs as accelerometers throughout the remainder of this chapter.

2.2.4 Digitally Reconstructed Radiographs

For spatially accurate DRR generation, calculation of the C-Arm pose with respect to the phantom was required. We used a scaled down mannequin model as our phantom and placed it on a fixed position on the table (which we knew from construction to be the center of the C-Arm gantry) and defined this as the physical coordinate system origin (see Fig. 2.5).

---

[4] https://plustoolkit.github.io/

Figure 2.4: The WitMotion Inertial Measurement Unit (image courtesy of Wit-motion).

The C-Arm radius, gear ratios, and BaseToOrigin distance were also known from our Computer Assisted Design (CAD) model and we used these values along with the orientation values obtained from the accelerometers to calculate the C-Arm pose as follows:

$$T_{Source} \;=\; T_{Rad} T_{A1XY} T_{Wag} T_{A2X} T_V^R T_D^S \tag{2.1}$$

$$T_{Wag} \;=\; -T_O^B T_{A3Y} T_O^B \tag{2.2}$$

T_{Rad} is defined by the translation matrix

$$\begin{bmatrix} & & & 0 \\ & I_{3x3} & & 0 \\ & & & -Rad * 10 \\ 0 & 0 & 0 & 1 \end{bmatrix};$$

where Rad is the radius of the C-Arm. T_{A1XY} is defined by the concatenation of rotation matrices
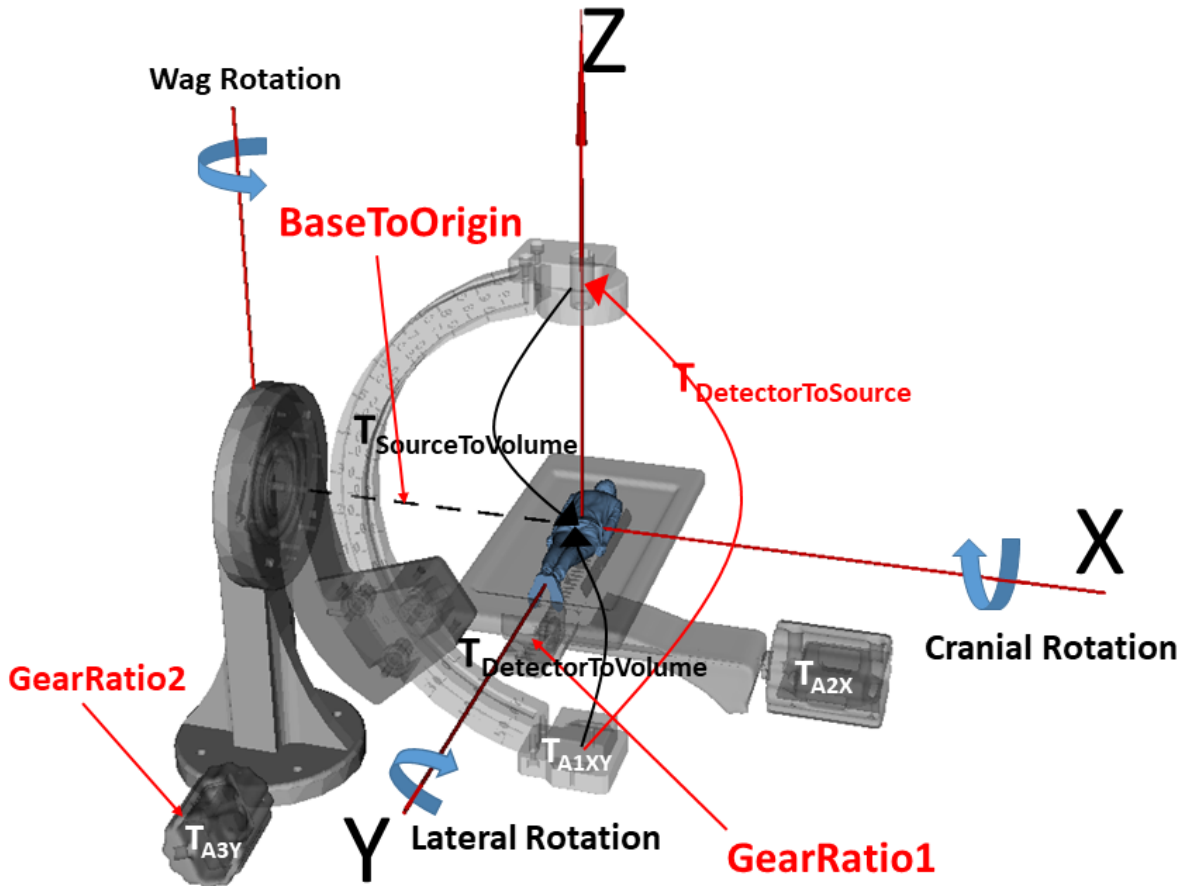
Figure 2.5: The physical coordinate system. Values known from construction are labelled in red.

$$\begin{bmatrix} 1 & 0 & 0 & 0 \\ 0 & cos(a1x) & -sin(a1x) & 0 \\ 0 & sin(a1x) & cos(a1x) & 0 \\ 0 & 0 & 0 & 1 \end{bmatrix} \begin{bmatrix} cos(a1y) & 0 & sin(a1y) & 0 \\ 0 & 1 & 0 & 0 \\ -sin(a1y) & 0 & cos(a1y) & 0 \\ 0 & 0 & 0 & 1 \end{bmatrix};$$

where a1x and a1y are the x and y orientation values obtained from accelerometer1, respectively. T_{A2X} is defined by the translation matrix

$$\begin{bmatrix} & & & 0 \\ I_{3x3} & & a2xg \\ & & & 0 \\ 0 & 0 & 0 & 1 \end{bmatrix};$$

where a2xg = accelerometer2's X Rotation/GearRatio1.

$T^R{}_V$ is the rotation required to align the axises of the physical coordinate system with the virtual coordinate system defined by

$$\begin{bmatrix} 0 & 1 & 0 & 0 \\ 0 & 0 & 1 & 0 \\ 1 & 0 & 0 & 0 \\ 0 & 0 & 0 & 1 \end{bmatrix};$$

$T^S{}_D$ is the source-to-detector transformation, which is a 180° rotation about the X axis defined by

$$\begin{bmatrix} 1 & 0 & 0 & 0 \\ 0 & -1 & 0 & 0 \\ 0 & 0 & -1 & 0 \\ 0 & 0 & 0 & 1 \end{bmatrix};$$

$T^B{}_O$ is defined by

$$\begin{bmatrix} & & & 10 * BtoO \\ I_{3x3} & & 0 \\ & & & 0 \\ 0 & 0 & 0 & 1 \end{bmatrix};$$

where BtoO is the known X distance from the Base of the C-Arm to the physical origin.

T_{A3YG} is defined by

$$\begin{bmatrix} cos(a3yg) & -sin(a3yg) & 0 & 0 \\ sin(a3yg) & cos(a3yg) & 0 & 0 \\ 0 & 0 & 1 & 0 \\ 0 & 0 & 0 & 1 \end{bmatrix};$$

where a3yg = accelerometer 3's y rotation/GearRatio2.

We used the calculated T_{Source} pose to position the virtual X-ray source, focal point, and "up" vector in the Visualization ToolKit (VTK)[5] coordinate space and positioned the CT volume at the origin. Real-time generation of the DRRs was achieved using the VTK GPU ray-tracing algorithm and a 1-dimensional colour and opacity transfer function that simulated the attenuation of X-rays in tissue. For this, we leveraged the Graphical User Interface (GUI) in the Slicer volume rendering module[6] and exported the volume property file for use in our application. This allowed us to have an expert clinician experimentally define the transfer function that best resembled the X-ray images most commonly used for training.

While this approach does not directly simulate the photon-matter interaction, as would be the case with a physics-based approach, it allows for the generation of high quality, real-time DRRs. The benefits of seeing how the DRR changes in real-time with respect to the movement of the C-Arm outweighed the benefits of more physically accurate images that do not render in real-time.

2.2.5 Software Application

The software was written in C++ and VTK. The system architecture diagram can be seen in Fig. 2.6. The DataRepository class deserializes the configuration file data via the Plus Toolkit, which is also used to interface with the accelerometers. The angular data are acquired from the accelerometers via a one-way serial port Bluetooth connection and pushed to the VisualizationController, which generates the DRRs and updates the GUI.

The primary feature of the system is the real-time visualization of DRRs based on the C-Arm position, as well as the corresponding evaluation mode in which the user must complete a number of rounds or 'levels' of image acquisitions. The system contains an administrator mode in which the user can customize the evaluation component of the software specifying the number of levels, the CT volume used for each level, and the ground truth C-Arm parameters (lateral rotation, cranial rotation, wag rotation, and table translation) for each level. Other

---

[5]https://vtk.org/
[6]https://www.slicer.org/wiki/Documentation/4.3/Modules/VolumeRendering
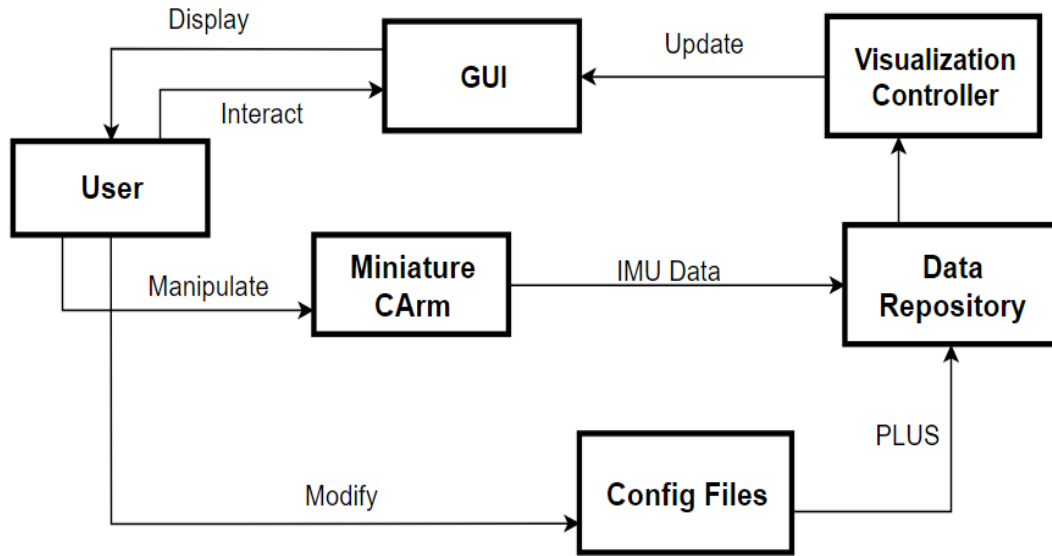
Figure 2.6: Software architecture. The DataRepository class is used to interface with the accelerometers and forward the angular data to the VisualizationController class for DRR generation.

features of the application include loading different CT volumes dynamically, customizing transfer function presets, and sliders to adjust the zoom and field-of-view. A screenshot of the GUI is shown in Fig. 2.7, and link to a video demo of the system can be found here[7].

2.2.6 User Study

We conducted a user study to evaluate the efficacy of the system as a training tool for lumbar spine injection procedures. We recruited 20 anesthesiology and orthopedic residents and divided them evenly into control and experimental groups. The experimental group was given the same evaluation task as the control group but received 5 minutes of prior training using the real-time DRR functionality of the system. Both groups received a 2 page curriculum on how to correctly position the C-Arm for 3 standard C-Arm views commonly used for lumbar spine procedures seen in Fig. 2.8: Full AP, Full Lateral and "Scotty Dog" (ideally 20° lateral rotation). The ground truth images with the corresponding C-Arm parameters (lateral rotation, cranial rotation, wag rotation, and table translation) used to obtain them were defined by an expert clinician with 20+ years of experience in spinal injection procedures. For the evaluation

---
[7]https://www.youtube.com/watch?v=HTMEmGuSuMk
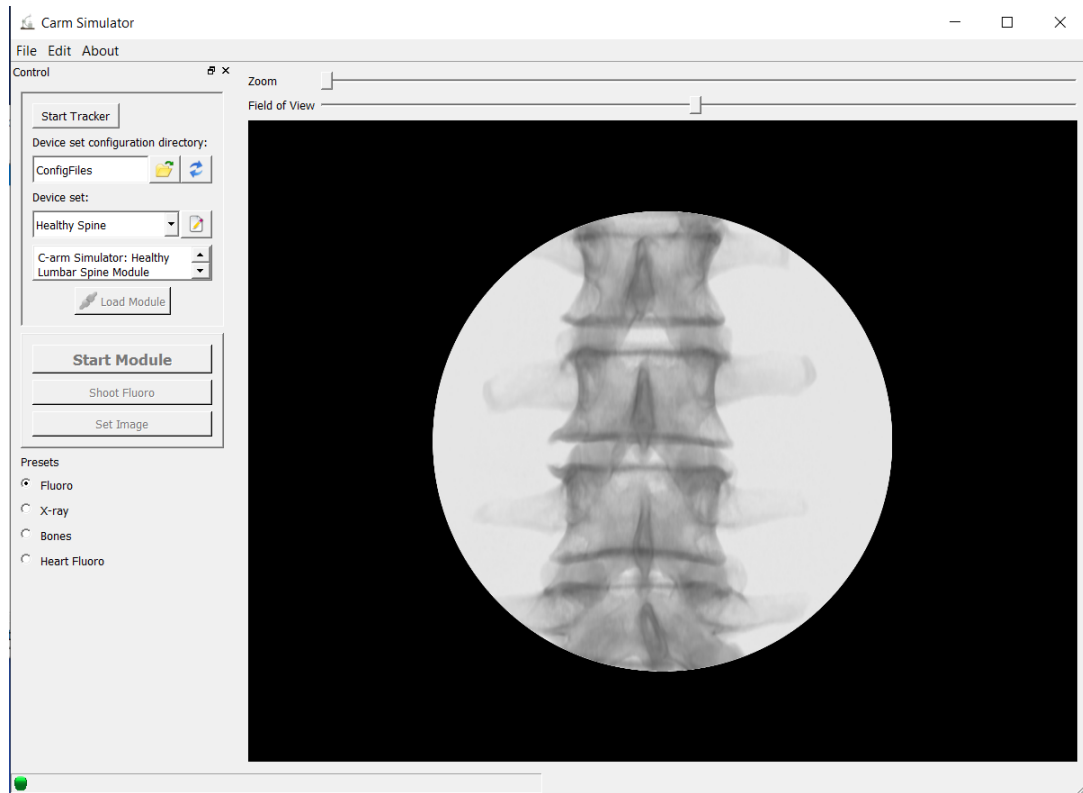
Figure 2.7: Screenshot of the GUI.

component, the users in both groups were required to take static DRR images (shots) using a foot-pedal to simulate the workflow of a typical spinal injection procedure. They were required to manipulate the C-Arm until they were satisfied with their acquired DRR. Each user performed 9 rounds of evaluation (3 for each view) with the order of the rounds presented to them at random. The volume was also randomly shifted slightly between each round to avoid memorization of the angles. The C-Arm parameters and total procedure time were recorded for each view. All participants also filled out a 5-point likert scale questionnaire to provide user experience feedback on the system.

2.3 Results

2.3.1 DRR Generation

The qualitative results from the DRR generation can be seen in Fig. 2.9. The system can generate the DRRs at a frame rate of 30 frames/second on a Windows 10 laptop equipped with a 2.5 GHz AMD A12-9700P Radeon R7 CPU, an AMD Radeon R7 graphics card, and 8 GB
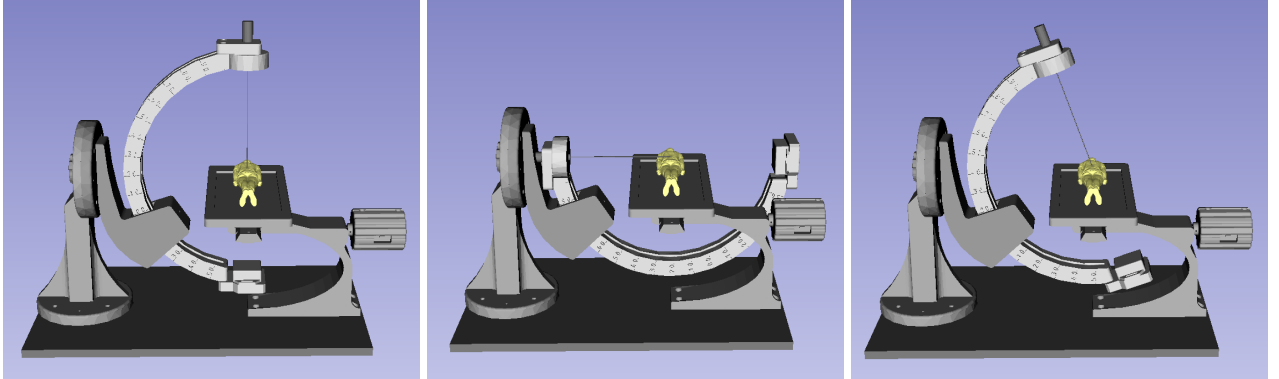
Figure 2.8: Three Standard Lumbar Spine C-Arm Views: Full AP, Full Lateral, and Scotty Dog (left to right)

of RAM.

Figure 2.9: The corresponding DRRs for the three Standard Lumbar Spine C-arm Views: Full AP, Full Lateral, and Scotty Dog (left to right)

2.3.2 User Study

The quantitative results from the study are shown in Fig 2.10. The experimental group achieved an C-Arm angular error and table translation error of $4.8 \pm 1.7°$ and 12.6 ± 5.1 mm respectively, which was significantly more accurate (angular: $p = 0.0029$, translational: $p = 0.0244$) than the control group at $6.9 \pm 3.7°$ and 16.9 ± 11 mm. The mean procedure time was 5.64 min for the experimental group which was significantly lower ($p = 0.046$) than the control group at 6.48 min. The p values were calculated using a T-test with the distribution mean set to the control group mean. The overall feedback of the system was positive, with the results from the Likert scale questionnaire shown in Table. 2.1
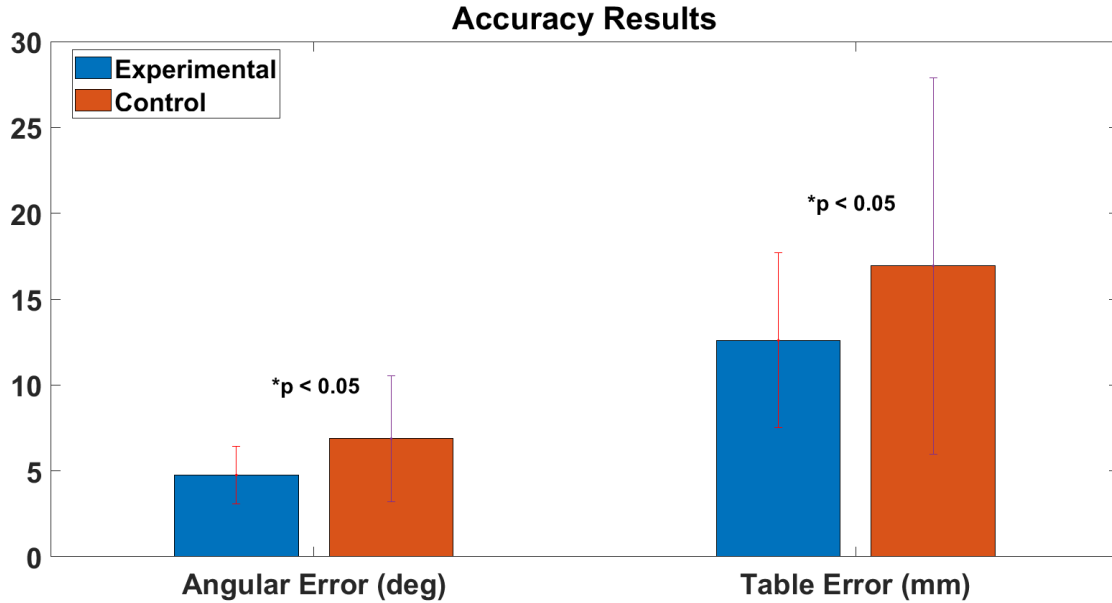
Figure 2.10: The mean accuracy results and standard deviation for each group.

Question	Mean Score
The simulator is user friendly	4.55
The simulator overall realistically represents fluoroscopy of the lumbar spine	4.80
The simulator is suitable for training novices	4.75
The simulator is suitable for training experts	4.15
Integration of simulator into medical education would be useful	4.85

Table 2.1: Questionnaire results (1 = Strongly Disagree, 2 = Disagree, 3 = Neutral, 4 = Agree, 5 = Strongly Agree).

2.4 Discussion

We developed a miniature C-Arm simulator and evaluated its efficacy as a training tool for interventional spine procedures. We saw significant improvement in C-Arm positioning ability after training on our system and received promising results in favour of the acceptance of cost-effective C-Arm training on a miniature model. The main advantage of our system compared to the others listed in table 1.2 is the accessibility it offers. Like the system proposed in [54], it does not require access to a physical C-Arm but instead provides a scaled down 3D-printed model. We have addressed some of the evaluation limitations of other approaches by providing qualitative evaluation through a likert scale questionnaire and quantitative feedback through an evaluation task. The evaluation task measured C-Arm positioning accuracy and total procedure

time, with the experimental group achieving significantly better results in both these areas compared to the control group.

Applications of our system include patient specific procedure planning, as well as the training of both clinicians and radiation technologists. The system allows for custom modules to be added via configuration files, where the user can specify the CT volume(s) and ground truth angles for the evaluation task. This feature enables trivial extendability into cardiac procedures, which are discussed in Sec. 4.1.3.

Future work includes incorporating a webcam-tracked needle to enable simulation of end-to-end spinal injection procedures. This would involve fixing trackable markers to the needle and phantom and registering them with the accelerometer-tracked C-Arm source. With the needle registered in the volume rendering coordinate space, a surface mesh of the needle can be incorporated intro the DRRs. Further discussion on the application, limitations, and future work of the miniature C-Arm simulator can be found in chapter 4.

Chapter 3

Open Source Virtual Reality C-Arm Simulator

3.1 Introduction

Chapter 2 focused on the development and evaluation of a miniature 3D-printed C-Arm simulator. The system provided the benefits of hands-on training with a physical simulator while remaining cost-effective and portable. However, the intended users for the system include medical students and residents, and due to their busy schedules, the requirement of a physical model might reduce the amount of use they would get out of the system compared to an entirely virtual approach.

C-Arm positioning training is well-suited for VR due to its highly visual learning-based nature. The difficulty that arises from this task stems not from the physical manipulation of the C-Arm, but the spatial mapping required from 2D fluoroscopic image to 3D C-Arm and patient. This training can be performed on a 2D desktop application [7], but then the spatial mapping becomes even more difficult as the user must reconstruct the 3D scene in their head from the 2D projection on the computer. Performing the training in a stereoscopic HMD gives the user 3D visualization and depth perception, and thus in theory the same degree of visual training they would receive in the real world.

For many VR applications, the learning curve associated with the skills for interaction is a bottleneck in the willingness for new users to adopt the technology. The muscle memory that computer users have for navigation on a standard computer via a mouse and keyboard does not exist for new users to VR technology. Because the proposed simulator can be used without the requirement of learning new complex skills, it allows users to focus on the visualization aspect without dwelling on the learning curve associated with complex interaction.

44

The VirtX VR simulator [48], proposes the concept of C-Arm training through a VR HMD environment. The system was evaluated very positively with 39 out of the 41 participants agreeing that C-Arm positioning is a highly relevant task for VR simulation. Their platform is built on Unity[1], which enables easy implementation of interaction, such as physical manipulation of the C-Arm by reaching and dragging with the controllers.

Although containing a higher degree of built-in support for VR, Unity does not offer the same capabilities as Slicer in the context of medical applications. The Slicer virtual reality module [2] (SlicerVR) [13] enables support for stereoscopic visualization in a HMD, enabling the integration of classic Slicer modules into a VR environment.

Building on the work from Chapter 2, we propose an immersive virtual reality system for the training of C-Arm manipulation. Our system is similar to [48] but built on the Slicer platform and tailored for fluoroscopy guided spine intervention (Fig. 3.1). Its benefits, when used in a training environment, are that it eliminates the need for a physical C-Arm and can be used in virtually any location as long as the user has access to the appropriate HMD. When combined with a magnetic tracking device [23], our proposed system has the ability to track a surgical needle although this feature is not discussed in this chapter.

3.2   Methods

Towards implementing an immersive VR environment of an Operating Room (OR) suite, with the capability to physically track surgical instruments, we developed a VR C-Arm simulator on top of the Slicer platform. Together with SlicerIGT [3] and SlicerVR, our system is compatible with a wide range of Head-Mounted Display systems including the HTC VIVE, Windows Mixed Reality headset, and Oculus Rift.

3.2.1   VR Engines

Common VR engines used for the gaming industry and medical application include Unity and SlicerVR. Unity's game engine provides a very intuitive interface for developing VR applications. Collision detection is built-in, making the physics behind interaction with virtual objects seamless. However, the open-source medical research modules that Slicer offers as well as the integration with tracking devices make Slicer the platform of choice for our system. The volume rendering module in Slicer generates realistic DRRs in real-time via a one—dimensional transfer function. The user has the ability to alter the transfer function dynamically using an

---

[1]https://unity.com/
[2]https://github.com/KitwareMedical/SlicerVirtualReality
[3]http://www.slicerigt.org/wp/
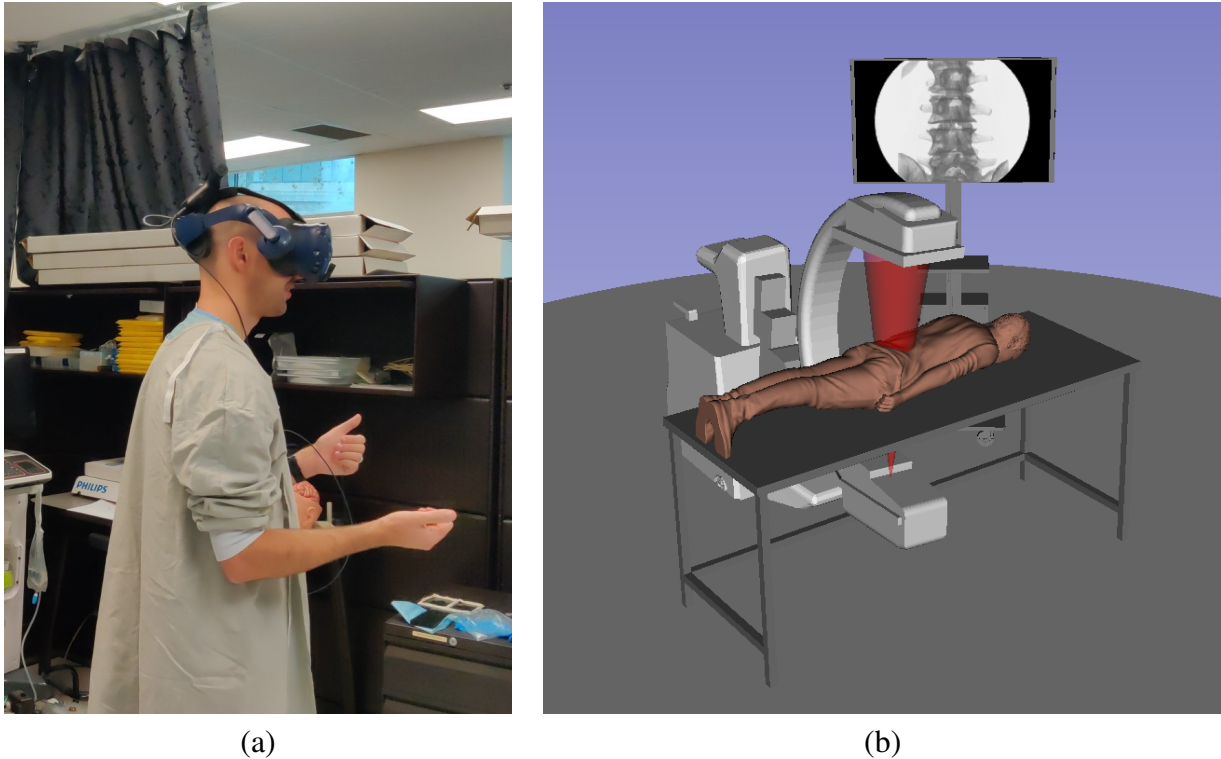
Figure 3.1: (a) A user wearing the VIVE Pro HMD using the proposed system. (b) A screenshot of the virtual scene.

intuitive GUI, allowing for easy customization of DRR generation for various C-Arm machines or settings. The SlicerIGT extension listens for events being broadcasted by various tracking devices such as the NDI Polaris (Northern Digital Inc., Canada) through the Plus server [4]. The SlicerVR extension exposes the transforms for the HMD, controllers, and any generic trackers associated with the HMD which integrates seamlessly with other modules. With a co-calibration mechanism [23], the internal tracking system of the HMD can be co-registered with the external tracking system used for tracked surgical instruments.

3.2.2   System Requirements and Hardware

The hardware requirements are dictated by the computational resources needed to drive the HMD system. In our implementation, we employed a Windows 10 Pro computer equipped with a 3.2 GHz Intel Core i7-8700 CPU with 32 GB of RAM. An HTC Vive Pro HMD was used for the development and testing of the system, but was demonstrated to be compatible with any SlicerVR-compatible HMD. As well as the HMD device, The Vive Pro hand controllers

---
[4]https://plustoolkit.github.io/

were used for controlling the C-Arm and a generic tracking device was used to anchor the VR scene (Fig. 3.2).
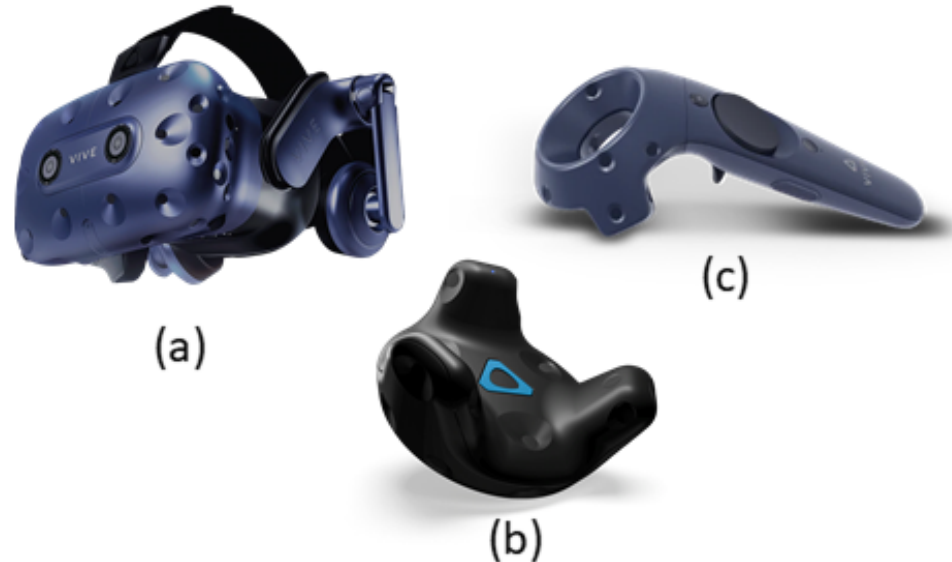
Figure 3.2: Vive Pro HMD (a), generic tracking device (b), and hand controller (c).

3.2.3 Virtual C-Arm

Most C-arms allow movement about 6 degrees of freedom (DoF): lateral rotation, cranial/caudal rotation, wag rotation and 3 translational DoFs. Typically only 4 DoFs are used for C-arm placement in spinal interventions: 3 rotational DoF and the posterior-anterior translation of the table (Fig. 3.4). We developed the system to allow for 6 DoF but for simplicity of the evaluation we restricted the movement to 4 DoF. We extracted the gantry, cranial/caudal support, and wag support components using SpaceClaim [5] from a 3D model of a C-arm taken from TurboSquid [6]. The surface representation of these support components were imported into Slicer.

3.2.4 Modelling C-Arm kinematics

The C-Arm kinematics were modelled by separating the C-Arm model into the three separate components (Fig. 3.3), and pairing each with the appropriate transforms:

---

[5] http://www.spaceclaim.com/en/default.aspx
[6] https://www.turbosquid.com/

$$Gantry = T_{Gantry}T_{CC}T_{Wag} \tag{3.1}$$

$$CCSupport = T_{Wag}T_{CC} \tag{3.2}$$

$$WagSupport = T_{Wag} \tag{3.3}$$
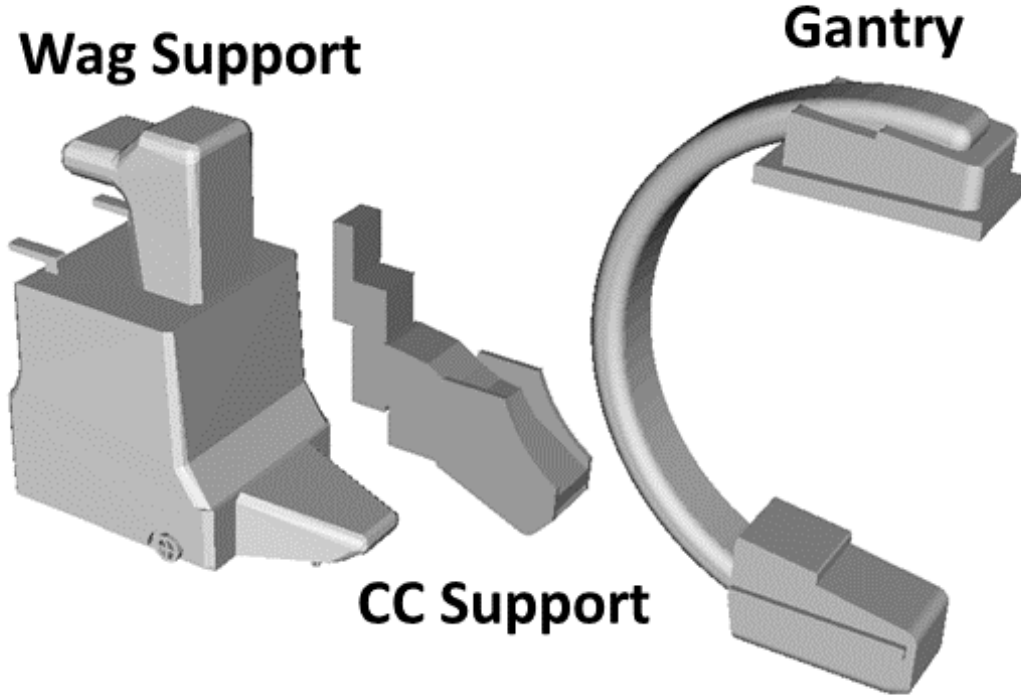
Figure 3.3: Extracted C-Arm components enabling to enable C-Arm DoFs.

.

3.2.5   DRR Generation

The DRRs were generated based on a patient CT and the pose of the virtual C-Arm. The pose of the C-Arm T_{Source} was calculated based on a method similar to the one described in Sec 2.2.4. The transforms required for this calculation are depicted in Fig. 3.4. The volume was placed at the C-Arm isocenter and the pose was calculated as follows:

$$T_{Source} = T_{Rad}T_{Gantry}T_{CC}T_{Wag}T_O^{Table} \tag{3.4}$$

$$T_{Wag} = -T_O^W T_Z T_O^W \tag{3.5}$$
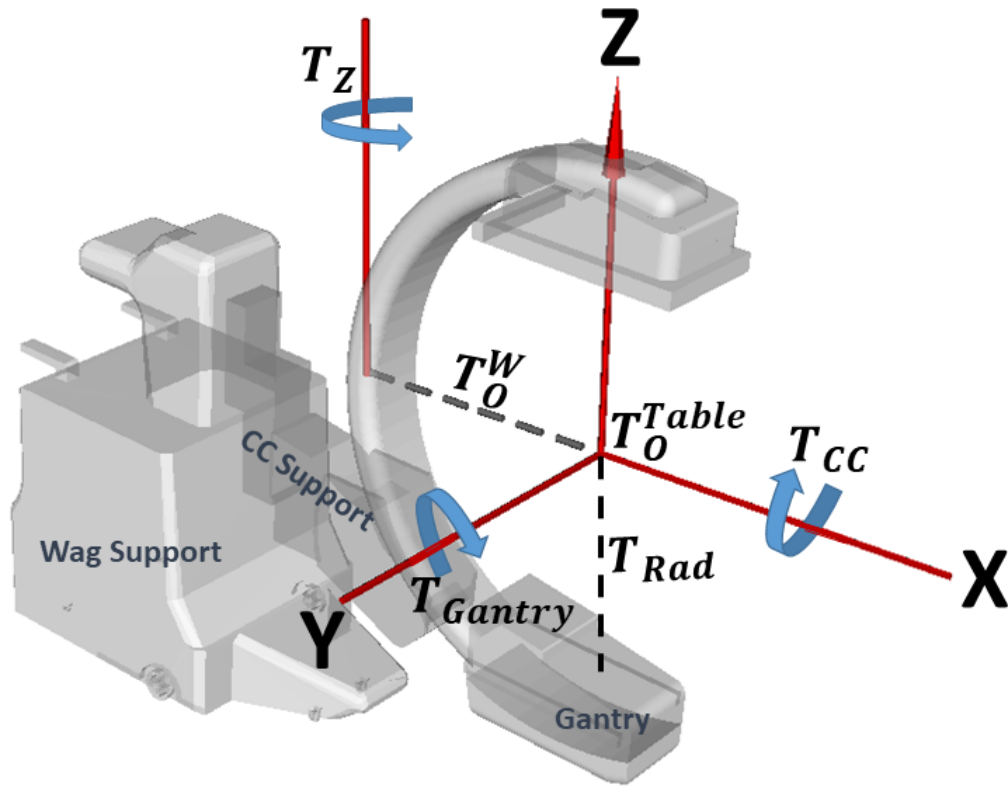
Figure 3.4: The transforms required to calculate the pose of the C-Arm source.

T_{Rad} is defined by the translation matrix

$$
\begin{bmatrix}
 & & & 0 \\
 & I_{3x3} & & 0 \\
 & & & -Rad \\
0 & 0 & 0 & 1
\end{bmatrix};
$$

where Rad is the radius of the C-Arm.

T_{Gantry} is defined by the rotation matrix

$$
\begin{bmatrix}
cos(y) & 0 & sin(y) & 0 \\
0 & 1 & 0 & 0 \\
-sin(y) & 0 & cos(y) & 0 \\
0 & 0 & 0 & 1
\end{bmatrix};
$$

where y is the applied lateral rotation in degrees.

T_{CC} is defined by the rotation matrix

$$
\begin{bmatrix}
1 & 0 & 0 & 0 \\
0 & cos(x) & -sin(x) & 0 \\
0 & sin(x) & cos(x) & 0 \\
0 & 0 & 0 & 1
\end{bmatrix};
$$

where x is the applied cranial/caudal rotation in degrees.

$T^{Table}{}_O$ is defined by the translation matrix

$$
\begin{bmatrix}
 & & & 0 \\
 & I_{3x3} & & t \\
 & & & 0 \\
0 & 0 & 0 & 1
\end{bmatrix};
$$

where t is the translation of the table in millimeters.

$T^W{}_O$ is defined by

$$
\begin{bmatrix}
 & & & WToO \\
 & I_{3x3} & & 0 \\
 & & & 0 \\
0 & 0 & 0 & 1
\end{bmatrix};
$$

where WToO is the distance from the Wag rotation axis to the origin.

T_Z is defined by

$$
\begin{bmatrix}
cos(z) & -sin(z) & 0 & 0 \\
sin(z) & cos(z) & 0 & 0 \\
0 & 0 & 1 & 0 \\
0 & 0 & 0 & 1
\end{bmatrix};
$$

where z is the applied wag rotation in degrees.

For DRR generation, we used a similar approach to the one described in 2.2.4, only this time the Slicer volume rendering module was used directly. In order to visualize the DRRs as a 2D image in the VR scene the CT volume was first rendered to an off-screen vtkRenderWindow object. We then extracted the 2D rendered image using the vtkWindowToImageFilter class and

displayed it as a textured plane in the scene. This pipeline is shown in Fig. 3.5.
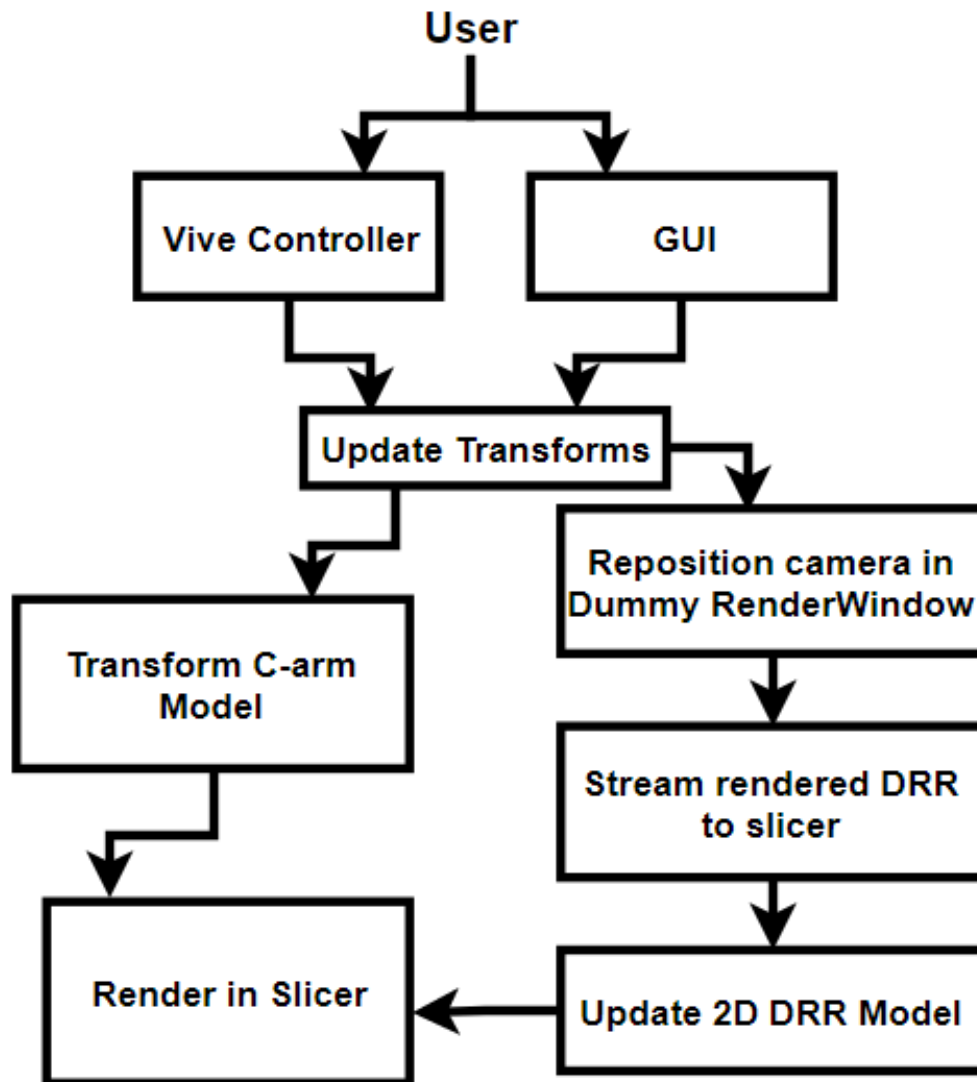
Figure 3.5: Flowchart depicting the DRR generation pipeline.

3.2.6 Slicer Module

A Slicer module was developed as the interface to control the zoom level, FOV, lateral rotation, cranial/caudal rotation, wag rotation, and table translation (see Fig. 3.6). Examples of different zoom and FOV configurations can be seen in Fig. 3.7. With Slicer as the VR engine, the scene can be easily customized for any surgical scenario. Using any SlicerVR-compatible HMD, the

user can view the scene in VR and manipulate the C-arm using the controllers. The code for the module can be found on github [7].

The module was designed for compatibility with other Slicer modules, to maximize its functionality and avoid duplicating code. The volume and volume property file (containing the transfer function parameters) are extracted from the volume rendering module directly to allow users to define the volume and transfer function using its GUI. The models (C-Arm, table, etc...) are contained in the resource folder of the module and are loaded upon press of the "Generate Scene" button. The user can modify or replace the models and save the new scene for subsequent uses. A link to a video demo of the system can be found here[8].
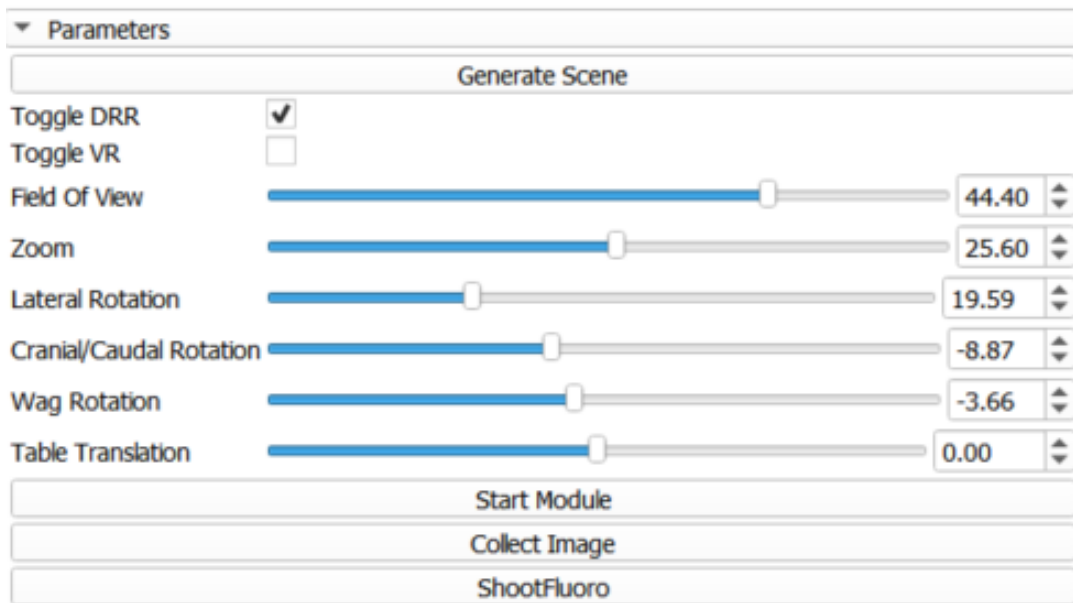
Figure 3.6: The Slicer module GUI.
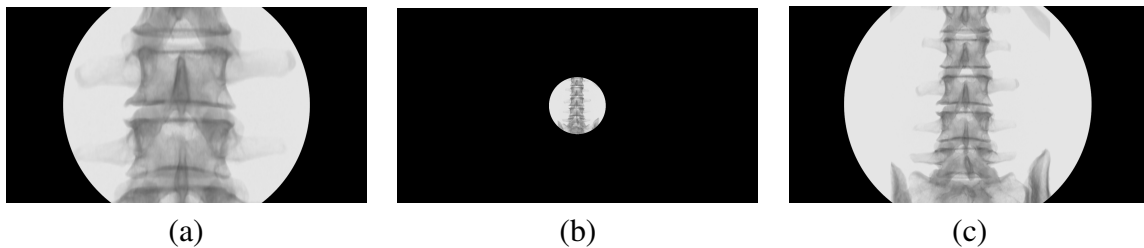
Figure 3.7: Examples of different Zoom and FOV configurations ((a) Zoom = 70%, FOV = 82%, (b) Zoom = 0%, FOV = 0%, (c) Zoom = 38%, FOV = 80%).

---

[7]https://github.com/dallen-28/CarmSimulatorSlicer
[8]https://www.youtube.com/watch?v=MRKUQ62UJ-s

3.2.7 System Architecture

An overview of the system architecture is depicted in Fig. 3.8. Events (transform data and controller actions) are sent through SteamVR and captured by the SlicerVR module which then forwards the data to the CarmSimulator module. The CarmSimulator module acts a controller, taking input from the user to compute and update the transforms accordingly. The models are then rendered in the Slicer scene. The scene is then extracted and split into stereo cameras by SlicerVR and finally sent back to SteamVR to be displayed in the HMD.
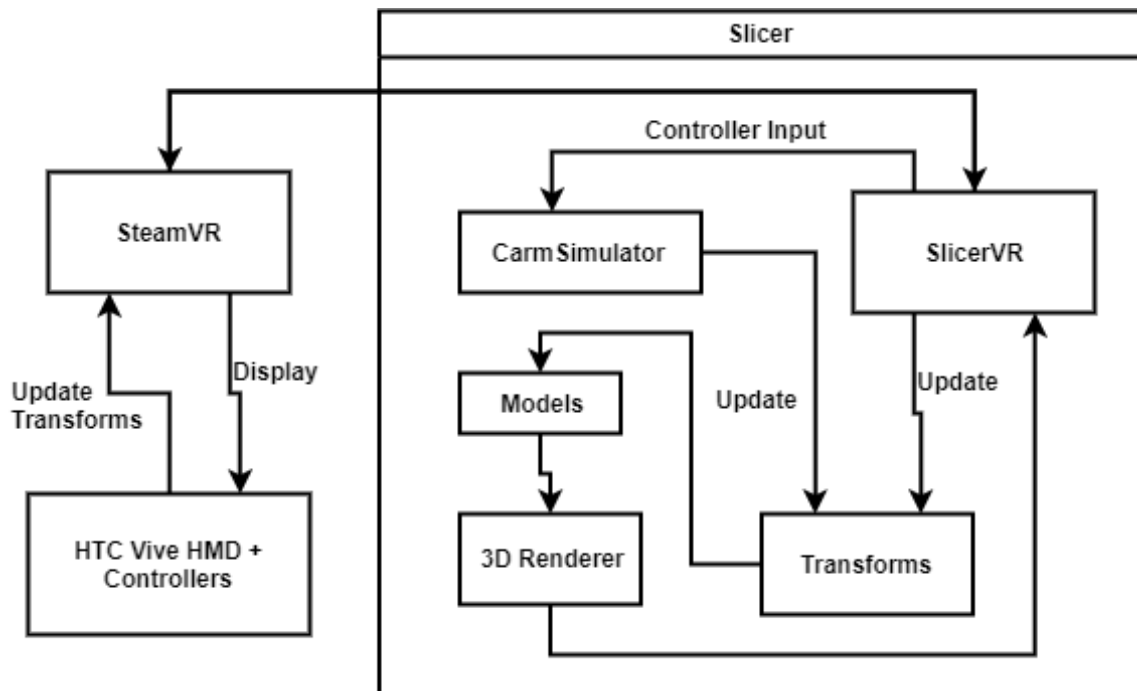
Figure 3.8: System Architecture. The Carm Simulator module acts as a controller to reformat the user input into the appropriate transforms to update the scene accordingly.

3.2.8 User Study

For initial validation and usability of the system, we recruited 2 experts and 5 graduate students to participate in a pilot study. Unfortunately, the recruitment of a larger cohort was hampered by the Covid-19 lockdown. The focus of this study was primarily to gain feedback via a 5-point Likert scale questionnaire. In addition, we also conducted an evaluation task in which the novice group was required to manipulate the C-Arm to obtain 3 standard fluoroscopic views commonly employed in interventional spinal procedures: Full AP, Full Lateral, and "Scotty Dog". The ground truth angles for these views were set by an expert clinician with more than 20 years of experience in pain management procedures. The ground truth images for these

three views based on a healthy spine were displayed to the user in the VR environment, and the users were required to obtain the matching view on a patient with a scoliotic spine using the displayed images as references. A semi-transparent red cone model was added to the scene and fixed to the C-Arm source to help the user visualize the target X-ray area. A screenshot of the scene from the user's perspective can be seen in Fig. 3.9.
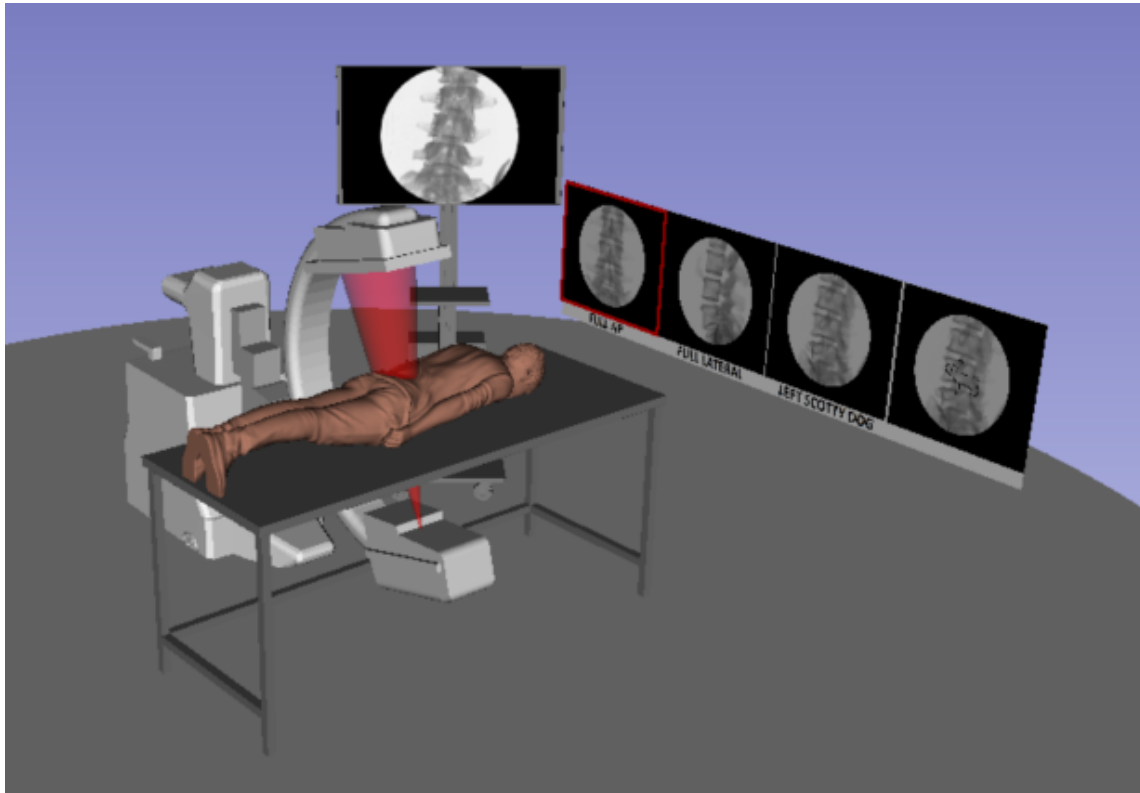
Figure 3.9: Screenshot of the evaluation component scene from the user's perspective.

3.2.9   Performance Metrics

Towards minimizing ionizing radiation exposure, the ALARA concept is used as the guiding principle for both medical training and surgical intervention [47]. To evaluate the performance of the participants, the following metrics were recorded: i) total procedural time, ii) angular and translation accuracy as compared to the gold standard set forth by the expert clinician, and iii) number of virtual fluoroscopic shots as a surrogate for the amount of x-ray exposure.

3.3 Results

3.3.1 User Study

angular error (in °)	translation error (in mm)	number of shots	total time
4.4 ± 2.0	30.3 ± 41.4	57.2 ± 14.9	18.9 ± 8.9 min
3.4 ± 1.4	3.4 ± 5.1		

Table 3.1: Novice user results. First row shows the results from all three views and the second row shows the results with the Full Lateral view acquisitions removed from the calculations.

The user performance results are shown in Table 3.1. The angular and translation results are reported by comparing the final pose of the C-Arm simulator to those defined by the clinical expert for the specified view. The overall feedback of the system was positive with the Likert scale questionnaire results shown in Tab. 3.2.

Question	Mean Score
The simulator realistically represents an X-ray image	4.8
The X-ray image is representative of the virtual C-Arm and patient position	5.0
Interaction with the C-Arm in the VR environment was user friendly	4.6
The simulator is suitable for training in novices	4.6
The simulator is suitable for training experts	4.0
Integration of simulator into medical education would be useful	4.5
Your spatial understanding of the movement of the C-Arm in VR was more intuitive than on a 2D display	4.5

Table 3.2: Likert scale (1 = Strongly Disagree, 2 = Disagree, 3 = Neutral, 4 = Agree, 5 = Strongly Agree).

3.4 Discussion

This chapter focused on the development of a Virtual Reality simulator for C-Arm positioning training in interventional spine procedures. A pilot study was conducted to evaluate its training capabilities and gain feedback on the overall user experience. Feedback from experts indicated high face and content validity of the simulator, and agreed on its potential as an effective training tool, but suggested areas of improvement. The user study saw reasonable C-Arm placement abilities in grad students after training on the system, however a follow-up study

will need to be conducted with a larger cohort of medical students and residents to identify its true efficacy as a training tool.

The proposed system serves as a training tool for both clinicians and MRTs. The MRT manipulates the C-Arm by adjusting the sliders on the GUI according to the clinician's verbal instructions. The MRT views the scene on the monitor and the clinician views the scene in the HMD. In "solo-player mode", the clinician can manipulate the C-Arm themselves using the hand controllers.

Aside from training, the intended application includes patient specific procedure planning. The user can dynamically load a CT volume and patient model to manually obtain the standard projections they will need for the procedure.

Because the clinician is wearing a fully occluded HMD, the inability to see the MRT with whom they are communicating with could serve as a potential source of error. The MRT can see the clinician but not their entire facial expression as it is blocked by the HMD. Assuming standardized medical terminology is used for relaying the instructions, these sight issues should not affect the team effort in positioning the C-Arm, but they still break away from a routine flow that the clinician and MRT might have in play.

Future work includes conducting a larger follow-up study to evaluate the training capabilities of our simulator compared to standard C-Arm training. We plan to recruit medical residents and experts as participants.

Towards simulation of end-to-end spinal procedures in VR, we plan to incorporate a physical spine model [36] and external spatial tracking system [23]. This will allow the user to insert a tracked needle into a physical spine, while getting both tactile and visual (2D DRR and 3D VR) feedback. The DRR generation will incorporate the real-time positioning of the needle.

Incorporating visualization of the user's hands is another potential feature in future versions of the system. To this end, two different methods of hand visualization have been explored which are discussed in Sec 4.2.3. Applications, limitations, and future work are discussed in more detail in the next chapter.

Chapter 4

Discussion and Conclusions

The following sections will focus on the applications, limitations and future work of the systems presented in chapters 2 and 3.

4.1 Miniature C-Arm

4.1.1 Applications

One of the primary applications where we believe that the miniature C-Arm simulator would yield the most benefits is in procedural planning. The system allows the pain management team to dynamically load in a patient's CT before the procedure to gain a better understanding of what C-Arm angles they will need for each particular view. The portability of the system allows this planning to be performed in virtually any location.

Another potential application of our system is in the training of both clinicians and MRTs. Understanding fluoroscopy and C-Arm kinematics through only theory-based education is extremely difficult due to its spatially complex nature. Hands-on training with our system could serve to be the perfect complement to theory-based education by allowing 3-dimensional visualization and interaction with a physical C-Arm model.

Competency-based education (CBE) is an emerging paradigm in the medical community as it serves as a more quantitative measurement for assessing the technical skills of medical students and residents. Charles *et al.* showed that a CBE program implemented in an elderly care program significantly improved residents training experience [12]. The C-Arm simulators proposed in this thesis fall in line nicely with the CBE model as they allow for a customizable training and evaluation environment, and serve as a means for quantitative C-Arm fluoroscopy skills assessment for medical students and residents.

4.1.2 Limitations

Using a 10:1 scaled down C-Arm, as opposed to a life-size model, has an obvious diminishing effect on the simulation capabilities. However, the angles used to produce identical DRRs will be the same for both models due to the principle of C-Arm rotation involving movement about the surface of a sphere.

The user study aiming to evaluate the system as a training tool showed that medical residents training on our system significantly outperformed the control group for the evaluation task. However the evaluation task was limited in the sense that it was performed on the miniature C-Arm and not on a scale C-Arm in a clinical setting. Having access to a physical C-Arm with real X-rays would serve as a better indicator of task performance, however due to ethical reasons we could not obtain this for our ground truth.

The use of accelerometers as a tracking modality was the best choice for our system albeit not without its limitations. We could only provide 4 out of the 6 possible DoFs and we needed three separate accelerometers to achieve that. We were also unable to easily incorporate a tracked needle into the system using an accelerometer as positional data is subject to drift.

4.1.3 Future Work

One potential solution for tracking the needle using the accelerometer would be via a calibration apparatus. This is inconvenient to the user however, and integrating other tracking modalities might provide for a better solution. In line with the objective to provide a cost-effective and portable device, we have also evaluated the use of webcam tracking technology. Initial results have shown promising potential and it is suspected that the incorporation of the needle will be integrated into the system as further research improves the underlying webcam tracking technology. The introduction of a tracked needle will enable end-to-end training for spinal injection procedures. This would involve 3D-printing a scale model of the patient's spine however, and the effects of the mismatch between the miniature C-Arm and scale phantom on the user are yet to be explored.

Support for four-dimensional (4D or time-series 3D) CT scans is a potential feature in future versions of the system that will expand its training capabilities into interventional cardiology by allowing for the visualization of the beating heart. We are also exploring techniques incorporating the effects of contrast agent flowing throughout the aorta and coronary arteries so that the system can be applied to cardiovascular medicine. To this end, we developed a simple console application that takes a CT volume and segmented labelmap as input, and increases the intensity of HU values at the locations in the CT corresponding to a user-defined label. Fig. 4.1 depicts the visualization benefits this contrast enhancement adds to a sample heart DRR.
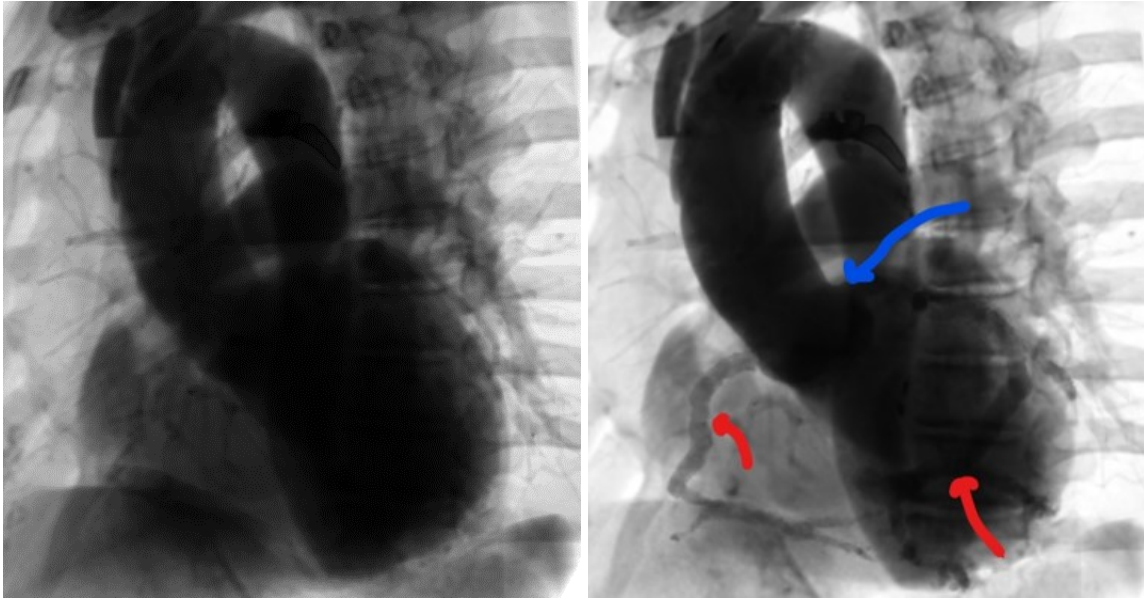
Figure 4.1: Heart DRR before contrast enhancement (left) and after running contrast enhancement algorithm (right). The Blue arrow points to the aorta and the red arrows point to the coronary arteries

4.2 VR C-Arm

4.2.1 Applications

Similar to the miniature C-Arm simulator, the VR version also serves as means of hands-on training without requiring access to a physical C-Arm. The only required equipment is a desktop computer with or without a HMD device.

Along with training for medical students and residents, the simulator also serves as a benefit to the patients as well. With the ability to view a VR simulation of the procedure they will be undergoing, it allows the patient to have a better understanding of the X-ray dose they will be exposed to, the details of the procedure, and the difficulty involved. The clinician can walk the patient through the procedure in an immersive environment, enabling a more effective means of communication, and potentially reducing the anxiety that is sometimes involved in the anticipation leading up to a procedure.

An entirely virtual training environment also allows for a high degree of customization. For example, the user can import their own X-ray monitor or operating table model and modify their positions to best simulate their desired training environment. With Slicer as the underlying platform, any of the modules can be incorporated into the scene. The volume rendering module allows dynamic customization of the transfer function through sliders in the GUI. They can simulate a multitude of C-Arm machine settings.

Interaction in a HMD VR environment can be a frustrating experience for new users. As opposed to their assumed ease of navigation on a standard desktop computer enabled by muscle memory built up over an extended period of time, their limited interaction skills in VR can hinder their ability to achieve the task as effectively as with a standard computer application. This often serves as a roadblock for the willingness of new users to accept VR as a replacement to standard 2D applications. Systems involving limited interaction, such as the proposed C-Arm simulator, may offer a better introduction to VR technology as they allow the user to focus on the unique visualization benefits of VR without dwelling on the frustrations. As they gain familiarity with the VR technology, the motivation to gain the interaction skills increases.

One initial unforeseen potential application of our system is in a training data generator for DRR generation neural networks [52]. The network proposed in [31] serves the purpose of automatically reporting C-Arm pose updates required to obtain a standard projection view. The network is trained by comparing arbitrarily defined planes in the CT volume to the standard projection plane defined by an expert clinician. The evaluation mode of our system innately records the difference in manually acquired C-Arm poses with the expert defined ground truth pose, consequently creating a large database of robust training data.

4.2.2 Limitations

While our system incorporates the use of hand controllers as a means to manipulate the virtual C-Arm, we made a design decision to control the pose of the C-Arm using the 2D widgets in Slicer via a human operator. This was based on the fact that, in the clinical setting, the clinicians generally do not manipulate the C-Arm directly. Instead, they provide voice instructions, using standardized medical terminology, to MRTs. Furthermore, the communication between the clinician and MRT is critical as smooth C-Arm adjustment and X-ray acquisition relies on the skills of the MRTs themselves[49]. While our experimental setup mimics the surgical scenario, the verbal communication between the clinician to the operator nonetheless has the potential for a source of error. For the full evaluation of our system, we plan to provide a more comprehensive training protocol to the participants, to allow more effective communication between the participants and the C-Arm operator.

The use of Slicer for the underlying VR platform has some limitations compared to using other more mature VR engines, such as Unity. Many of the physics features built-in to Unity such as collision detection and gravity are not included in the Slicer modules, making it more difficult to simulate a real-world environment. For example, at the moment Slicer does not provide collision detection, and strategic placing of the models in the scene is currently the only way to avoid objects clipping into each other. However, Slicer still has significant advantages

over Unity in the realm of medical imaging. The ability to combine modules in Slicer, either through the GUI or programmatically, allow for a more customizable simulation environment for medical VR training.

4.2.3   Future Work

The efficacy of our system is limited by two main factors: i) the number and type of the participants to demonstrate, with significance, the efficacy of our system, and ii) the technical limitation of our proposed HCI components. An REB for a follow-up study has been approved, in which we plan to recruit a sufficient number of participants with medical backgrounds (medical residents). These participants will be divided into a control and an experimental group, where the control group will receive standard training (as mandated by the residency training program). The experimental group will be trained using our proposed VR system, and our hypothesis is that the users trained on our VR system will achieve better accuracy in less time as compared to the control group. Our hypothesis is supported by the work of Touchette [49]. The ability to perform this study prior to submission of the thesis was unfortunately prevented by the COVID-19 shutdown.

Our current system is limited in that while it delivers a realistic DRR based on the current pose of the C-Arm, the image does not display a needle or other surgical instruments. Future work involves incorporating a physical phantom and external tracking system using the co-calibration apparatus proposed in [23]. This apparatus defines a rigid relationship between a tracker dynamic reference frame and the vive controller to enable the co-registration of physical and virtual environments. The tracked needle will be incorporated into the DRR generation pipeline, enabling the user to perform needle insertion procedures using the DRR image for guidance. The physical phantom will, simultaneously, allow the user to receive realistic haptic feedback.

A study by Groves *et al.* analyzing the use of a HMD for central venous catheterization showed that most users lose spatial awareness and coordination in a VR surgical environment without the sight of their hands [22]. We have experimented with two different technologies to help mitigate this issue. The first potential solution involves augmenting the virtual scene with real world objects such as the surgeon's hands and patient via the use of a stereo video cameras attached to the front of the HMD. The other potential solution is the incorporation of the Leap Motion infrared hand tracker [1]. The Leap Motion tracker tracks the location of finger digits and has been added as a new device to the Plus Toolkit, enabling integration into Slicer. Incorporating hand tracking into the system also enables the use of hand gesture recognition in

---

[1]https://www.leapmotion.com/

the system using the SlicerGestureRecognition module [2]. This module allows a user to train a variety of machine learning models to recognize various hand gestures based on the streaming transform data and then make real-time predictions as to the nature of the gesture. Interaction in a VR environment is currently limited and we expect that gesture recognition will become a valuable tool as VR surgical training programs become more widespread.

4.3 Conclusions

C-Arms have enabled the progressive development of many fluoroscopy-guided spinal procedures. In the past decades, the C-Arm has gained worldwide acceptance and enabled procedures to be successfully performed with a much lower radiation exposure than CT-guidance. However, the success of these procedures is highly dependent on accurate X-ray image acquisition which requires accurate positioning of the C-Arm with respect to the patient. Often, acquiring these images induces an increase of radiation exposure to both the clinician and patient, especially if the clinician does not have extensive experience. This experience typically comes from apprenticeship-based programs and cadaver training, but mostly from theoretical knowledge. Hands on training for C-Arm procedures has been extensively explored and has been addressed through the use of radiation-free simulators. These simulators however are still limited in their accessibility and validation for training.

To this end we developed a miniature 3D-printed C-Arm simulator which is presented in Chapter 2. This simulator is capable of producing real-time DRRs based on the pose of the C-Arm source, which is tracked in space via Bluetooth accelerometers. Although geared towards lumbar spine procedures, we developed the system with the context of customizable C-Arm training in mind, not limiting the application to a single procedure. The system was evaluated by conducting a user study split up into experimental and control groups, with both groups performing a C-Arm positioning evaluation task on the simulator but with the experimental group receiving 5 minutes of training prior to the evaluation task. The total procedure time, angular and translation accuracy were measured to quantify the benefits of training on the simulator. The experimental group achieved significantly higher accuracy and lower total procedure time than the control group. Both groups filled out a 5-pt likert scale questionnaire to report on the overall user experience and acceptance of the simulator into standard medical education. The questionnaire was received with positive results, indicating high potential for successful adoption of the simulator into the clinic.

Chapter 3 expands upon the idea of accessible C-Arm training through the use of an entirely virtual C-Arm simulator. The system offers an immersive training experience through the

---

[2] `https://github.com/VASST/SlicerLeapMotion/tree/master/GestureRecognition`

visualization of a 3D C-Arm computer model and 2D virtual DRR display. Interaction is offered through the use of VR hand controllers or sliders on the GUI to be operated by a secondary user. The system was primitively evaluated by students and 2 expert clinicians with promising results, however a follow-up study will need to be conducted to gain significant results on the efficacy of the system as a training tool.

This thesis focused on two novel simulation systems, both addressing pitfalls of previous approaches of C-Arm simulation for training. Both approaches have their limitations, but offer promising solutions for accessible, hands-on training systems.

As VR technology continues to evolve, the potential techniques for increasing the immersion are endless. HMDs will become cheaper and more lightweight and as interaction in a VR environment evolves, they will slowly start replacing standard computers for applications in which 3D visualization has inherent benefits.

Appendix A

Copyright Transfers and Reprint Permissions

The reprint permissions for the following accepted articles are provided:

- CT fluoroscopy–guided epidural injections: technique and results [55].

  - reprint authorized from the American Journal of NeuroRadiology with request ID 600019860.

- Comparison of measurements of mandible growth using cone beam computed tomography and its synthesized cephalogram [34].

  - reprint authorized from Springer Nature with license number 4881131035461.

All other copyright material is under sole ownership by the author, including arXiv pre-prints, and articles currently under submission or revision.

Bibliography

[1] Daniel R Allen, John Moore, Abigayel Joschko, Collin Clarke, Terry M Peters, and Elvis CS Chen. Miniature C-Arm simulator using wireless accelerometer based tracking. In *Medical Imaging 2020: Image-Guided Procedures, Robotic Interventions, and Modeling*, volume 11315, page 1131502. International Society for Optics and Photonics, 2020.

[2] Andreu Badal and Aldo Badano. Accelerating monte carlo simulations of photon transport in a voxelized geometry using a massively parallel graphics processing unit. *Medical Physics*, 36(11):4878–4880, 2009.

[3] Bastian Bier, Mathias Unberath, Jan-Nico Zaech, Javad Fotouhi, Mehran Armand, Greg Osgood, Nassir Navab, and Andreas Maier. X-ray-transform invariant anatomical landmark detection for pelvic trauma surgery. In *International Conference on Medical Image Computing and Computer-Assisted Intervention*, volume 11073, pages 55–63. Springer, 2018.

[4] Wolfgang Birkfellner, Rudolf Seemann, Michael Figl, Johann Hummel, Christopher Ede, Peter Homolka, Xinhui Yang, Peter Niederer, and Helmar Bergmann. Fast DRR generation for 2D/3D registration. In *International Conference on Medical Image Computing and Computer-Assisted Intervention*, volume 3750, pages 960–967. Springer, 2005.

[5] Flemming Bjerrum, Ann Sofia Skou Thomsen, Leizl Joy Nayahangan, and Lars Konge. Surgical simulation: current practices and future perspectives for technical skills training. *Medical teacher*, 40(7):668–675, 2018.

[6] Thomas R. Blattert, Ute A. Fill, Elmar Kunz, Werner Panzer, Arnulf Weckbach, and Dieter F. Regulla. Skill dependence of radiation exposure for the orthopaedic surgeon during interlocking nailing of long-bone shaft fractures: a clinical study. *Archives of Orthopaedic and Trauma Surgery*, 124(10):659–664, 2004.

[7] OJ Bott, M Teistler, C Duwenkamp, M Wagner, M Marschollek, M Plischke, BW Raab, KM Stürmer, DP Pretschner, and K Dresing. Virtx–evaluation of a computer-based training system for mobile C-Arm systems in trauma and orthopedic surgery. *Methods of information in medicine*, 47(03):270–278, 2008.

[8] Oliver Johannes Bott, Klaus Dresing, Markus Wagner, Björn-Werner Raab, and Michael Teistler. Informatics in radiology: use of a C-Arm fluoroscopy simulator to support training in intraoperative radiography. *Radiographics*, 31(3):E65–E75, 2011.

[9] Oliver Johannes Bott, Markus Wagner, Christopher Duwenkamp, Nils Hellrung, and Klaus Dresing. Improving education on C-Arm operation and radiation protection with a computer-based training and simulation system. *International journal of computer assisted radiology and surgery*, 4(4):399–407, 2009.

[10] David J Brenner, Carl D Elliston, Eric J Hall, and Walter E Berdon. Estimated risks of radiation-induced fatal cancer from pediatric CT. *American journal of roentgenology*, 176(2):289–296, 2001.

[11] Wenli Cai and Georgios Sakas. DRR volume rendering using splatting in shear-warp context. In *2000 IEEE Nuclear Science Symposium. Conference Record (Cat. No. 00CH37149)*, volume 3, pages 19–12. IEEE, 2000.

[12] Lesley Charles, Jean Triscott, Bonnie Dobbs, Peter George Tian, and Oksana Babenko. Effectiveness of a core-competency–based program on residents' learning and experience. *Canadian Geriatrics Journal*, 19(2):50, 2016.

[13] Saleh Choueib. Virtual reality in 3D Slicer. In *Inquiry@ Queen's Undergraduate Research Conference Proceedings*, 2019.

[14] Tharindu De Silva, J Punnoose, Ali Uneri, Joseph Goerres, M Jacobson, Michael D Ketcha, Amir Manbachi, Sebastian Vogt, Gerhard Kleinszig, Akhil J Khanna, et al. C-Arm positioning using virtual fluoroscopy for image-guided surgery. In *Medical Imaging 2017: Image-Guided Procedures, Robotic Interventions, and Modeling*, volume 10135, page 101352K. International Society for Optics and Photonics, 2017.

[15] Philipp Dressel, Lejing Wang, Oliver Kutter, Joerg Traub, Sandro-Michael Heining, and Nassir Navab. Intraoperative positioning of mobile C-Arms using artificial fluoroscopy. In *Medical Imaging 2010: Visualization, Image-Guided Procedures, and Modeling*, volume 7625, page 762506. International Society for Optics and Photonics, 2010.

[16] Andinet Enquobahrie, Patrick Cheng, Kevin Gary, Luis Ibanez, David Gobbi, Frank Lindseth, Ziv Yaniv, Stephen Aylward, Julien Jomier, and Kevin Cleary. The image-guided surgery toolkit IGSTK: an open source c++ software toolkit. *Journal of digital imaging*, 20(1):21–33, 2007.

[17] Nancy E Epstein. The risks of epidural and transforaminal steroid injections in the spine: Commentary and a comprehensive review of the literature. *Surgical neurology international*, 4(Suppl 2):S74, 2013.

[18] FJ Falco, Laxmaiah Manchikanti, Sukdeb Datta, Nalini Sehgal, Stephanie Geffert, Obi Onyewu, Vijay Singh, David A Bryce, Ramsin M Benyamin, Thomas T Simopoulos, et al. An update of the systematic assessment of the diagnostic accuracy of lumbar facet joint nerve blocks. *Pain Physician*, 15(6):E869–E907, 2012.

[19] Javad Fotouhi, Bernhard Fuerst, Alex Johnson, Sing Chun Lee, Russell Taylor, Greg Osgood, Nassir Navab, and Mehran Armand. Pose-aware C-arm for automatic re-initialization of interventional 2D/3D image registration. *International Journal of Computer Assisted Radiology and Surgery*, 12(7):1221–1230, 2017.

[20] Afshin Gangi, Jean-Louis Dietemann, Reza Mortazavi, Dominique Pfleger, Christian Kauff, and Catherine Roy. CT-guided interventional procedures for pain management in the lumbosacral spine. *Radiographics*, 18(3):621–633, 1998.

[21] Ren Hui Gong, Brad Jenkins, Raymond W Sze, and Ziv Yaniv. A cost effective and high fidelity fluoroscopy simulator using the image-guided surgery toolkit (IGSTK). In *Medical Imaging 2014: Image-Guided Procedures, Robotic Interventions, and Modeling*, volume 9036, page 903618. International Society for Optics and Photonics, 2014.

[22] Leah Groves, Natalie Li, Terry M. Peters, and Elvis C. S. Chen. Towards a mixed-reality first person point of view needle navigation system. In Dinggang Shen, Tianming Liu, Terry M. Peters, Lawrence H. Staib, Caroline Essert, Sean Zhou, Pew-Thian Yap, and Ali Khan, editors, *Medical Image Computing and Computer Assisted Intervention – MICCAI 2019*, volume 11768, 2019.

[23] Leah A. Groves, Patrick Carnahan, Daniel R. Allen, Rankin Adam, Terry M. Peters, and Elvis C.S. Chen. Accuracy assessment for the co-registration between optical and VIVE head-mounted display tracking. *International Journal of Computer Assisted Radiology and Surgery*, 14(7):1207–1215, 2019.

[24] Victor Grzeda and Gabor Fichtinger. C-Arm rotation encoding with accelerometers. *International journal of computer assisted radiology and surgery*, 5(4):385–391, 2010.

[25] Jonas Hajek, Mathias Unberath, Javad Fotouhi, Bastian Bier, Sing Chun Lee, Greg Osgood, Andreas Maier, Mehran Armand, and Nassir Navab. Closing the calibration loop: an inside-out-tracking paradigm for augmented reality in orthopedic surgery. In *International Conference on Medical Image Computing and Computer-Assisted Intervention*, volume 11073, pages 299–306. Springer, 2018.

[26] Mustafa Hussein and Carl Nätterdal. The benefits of virtual reality in education-a comparision study. 2015.

[27] Giorgio Ivani and F Michael Ferrante. American society of regional anesthesia and pain medicine and the European society of regional anaesthesia and pain therapy joint committee recommendations for education and training in ultrasound guided regional anesthesia: Why do we need these guidelines? *Regional anesthesia and pain medicine*, 34(1):8, 2009.

[28] Ameet Jain and Gabor Fichtinger. C-Arm tracking and reconstruction without an external tracker. In *International Conference on Medical Image Computing and Computer-Assisted Intervention*, volume 4190, pages 494–502. Springer, 2006.

[29] Ameet Kumar Jain, Tabish Mustafa, Yu Zhou, Clif Burdette, Gregory S Chirikjian, and Gabor Fichtinger. Ftrac—a robust fluoroscope tracking fiducial. *Medical physics*, 32(10):3185–3198, 2005.

[30] Haemi Jee, Ji Hae Lee, Jongwoo Kim, Ki Deok Park, Woo Yong Lee, and Yongbum Park. Ultrasound-guided selective nerve root block versus fluoroscopy-guided transforaminal

block for the treatment of radicular pain in the lower cervical spine: a randomized, blinded, controlled study. *Skeletal radiology*, 42(1):69–78, 2013.

[31] Lisa Kausch, Sarina Thomas, Holger Kunze, Maxim Privalov, Sven Vetter, Jochen Franke, Andreas H Mahnken, Lena Maier-Hein, and Klaus Maier-Hein. Toward automatic C-Arm positioning for standard projections in orthopedic surgery. *International Journal of Computer Assisted Radiology and Surgery*, pages 1–11, 2020.

[32] Mayumi Kitagawa and Yuzuru Kouno. *Development of X-Ray Fluoroscopy Devices*, pages 9–12. Springer Singapore, Singapore, 2017.

[33] Xiaoliang Li, Jie Yang, and Yuemin Zhu. Digitally reconstructed radiograph generation by an adaptive monte carlo method. *Physics in Medicine & Biology*, 51(11):2745, 2006.

[34] Hsien-Shu Lin, Jia-Da Li, Yunn-Jy Chen, Cheng-Chung Lin, Tung-Wu Lu, and Mu-Hsiung Chen. Comparison of measurements of mandible growth using cone beam computed tomography and its synthesized cephalograms. *Biomedical engineering online*, 13(1):133, 2014.

[35] William C McGaghie, Timothy J Draycott, William F Dunn, Connie M Lopez, and Dimitrios Stefanidis. Evaluating the impact of simulation on translational patient outcomes. *Simulation in healthcare: Journal of the Society for Simulation in Healthcare*, 6(Suppl):S42, 2011.

[36] A. Jonathan McLeod, John S. H. Baxter, Golafsoun Ameri, Sugantha Ganapathy, Terry M. Peters, and Elvis C. S. Chen. Detection and visualization of dural pulsation for spine needle interventions. *International Journal of Computer Assisted Radiology and Surgery*, 10(6):947–958, 2015.

[37] Samer N Narouze. *Atlas of ultrasound-guided procedures in interventional pain management*. Springer, 2018.

[38] Nassir Navab, Sandro-Michael Heining, and Joerg Traub. Camera augmented mobile C-Arm (camc): calibration, accuracy study, and clinical applications. *IEEE transactions on medical imaging*, 29(7):1412–1423, 2009.

[39] Stefania Pallotta and Marta Bucciolini. A simple method to test geometrical reliability of digital reconstructed radiograph (DRR). *Journal of applied clinical medical physics*, 11(1):287–291, 2010.

[40] Axel Pinz, Markus Brandner, Harald Ganster, Albert Kusej, Peter Lang, and Miguel Ribo. Hybrid tracking for augmented reality. *Ögai Journal*, 21(1):17–24, 2002.

[41] Morris Edgar Rose. *Elementary theory of angular momentum*. Courier Corporation, 1995.

[42] Andreas G. Schreyer and Simon K. Warfield. *Surface Rendering*, pages 31–34. Springer Berlin Heidelberg, Berlin, Heidelberg, 2002.

[43] J Anthony Seibert. Flat-panel detectors: how much better are they? *Pediatric radiology*, 36(2):173, 2006.

[44] Aaron Sodickson, Pieter F Baeyens, Katherine P Andriole, Luciano M Prevedello, Richard D Nawfel, Richard Hanson, and Ramin Khorasani. Recurrent ct, cumulative radiation exposure, and associated radiation-induced cancer risks from ct of adults. *Radiology*, 251(1):175–184, 2009.

[45] Nilam J Soni, Ricardo Franco-Sadud, Daniel Schnobrich, Ria Dancel, David M Tierney, Gerard Salame, Marcos I Restrepo, and Paul McHardy. Ultrasound guidance for lumbar puncture. *Neurology: Clinical Practice*, 6(4):358–368, 2016.

[46] Philipp Stefan, Séverine Habert, Alexander Winkler, Marc Lazarovici, Julian Fürmetz, Ulrich Eck, and Nassir Navab. A mixed-reality approach to radiation-free training of C-Arm based surgery. In *International Conference on Medical Image Computing and Computer-Assisted Intervention*, volume 10434, pages 540–547. Springer, 2017.

[47] Keith J. Strauss and Sue C. Kaste. The ALARA (as low as reasonably achievable) concept in pediatric interventional and fluoroscopic imaging: striving to keep radiation doses as low as possible during fluoroscopy of pediatric patients—a white paper executive summary. *Pediatric Radiology*, 36(S2):110–112, 2006.

[48] Matthias Süncksen, Henner Bendig, Michael Teistler, Markus Wagner, Oliver Johannes Bott, and Klaus Dresing. Gamification and virtual reality for teaching mobile x-ray imaging. In *2018 IEEE 6th International Conference on Serious Games and Applications for Health (SeGAH)*, pages 1–7. IEEE, 2018.

[49] Michèle Touchette. *Artificial X-ray imaging system (AXIS)–design and evaluation on C-Arm performance in operating room and educational settings*. PhD thesis, University of British Columbia, 2017.

[50] Mathias Unberath, Javad Fotouhi, Jonas Hajek, Andreas Maier, Greg Osgood, Russell Taylor, Mehran Armand, and Nassir Navab. Augmented reality-based feedback for technician-in-the-loop C-Arm repositioning. *Healthcare technology letters*, 5(5):143–147, 2018.

[51] Mathias Unberath, Jan-Nico Zaech, Cong Gao, Bastian Bier, Florian Goldmann, Sing Chun Lee, Javad Fotouhi, Russell Taylor, Mehran Armand, and Nassir Navab. Enabling machine learning in x-ray-based procedures via realistic simulation of image formation. *International journal of computer assisted radiology and surgery*, 14(9):1517–1528, 2019.

[52] Mathias Unberath, Jan-Nico Zaech, Sing Chun Lee, Bastian Bier, Javad Fotouhi, Mehran Armand, and Nassir Navab. DeepDRR–a catalyst for machine learning in fluoroscopy-guided procedures. In *International Conference on Medical Image Computing and Computer-Assisted Intervention*, volume 11073, pages 98–106. Springer, 2018.

[53] Tamas Ungi, Andras Lasso, and Gabor Fichtinger. Open-source platforms for navigated image-guided interventions. *Medical Image Analysis*, 33:181–186, 2016.

[54] Domenico Veneziano, Arthur Smith, Troy Reihsen, Jason Speich, and Robert M Sweet. The simportal fluoro-less C-Arm trainer: an innovative device for percutaneous kidney access. *Journal of Endourology*, 29(2):240–245, 2015.

[55] Andrew L Wagner. CT fluoroscopy–guided epidural injections: technique and results. *American journal of neuroradiology*, 25(10):1821–1823, 2004.

[56] Michael J Wallace, Michael D Kuo, Craig Glaiberman, Christoph A Binkert, Robert C Orth, Gilles Soulez, Technology Assessment Committee of the Society of Interventional Radiology, et al. Three-dimensional C-Arm cone-beam CT: applications in the interventional suite. *Journal of Vascular and Interventional Radiology*, 19(6):799–813, 2008.

[57] Lejing Wang, Simon Weidert, Joerg Traub, Sandro Michael Heining, Christian Riquarts, Ekkehard Euler, and Nassir Navab. Camera augmented mobile C-Arm. In *Bildverarbeitung für die Medizin 2009*, pages 97–101. Springer, 2009.

[58] Andrew D Wiles, David G Thompson, and Donald D Frantz. Accuracy assessment and interpretation for optical tracking systems. In *Medical Imaging 2004: Visualization, Image-Guided Procedures, and Display*, volume 5367, pages 421–432. International Society for Optics and Photonics, 2004.

[59] Thomas Wolff, Andras Lasso, Markus Eblenkamp, Erich Wintermantel, and Gabor Fichtinger. C-Arm angle measurement with accelerometer for brachytherapy: an accuracy study. *International journal of computer assisted radiology and surgery*, 9(1):137–144, 2014.

[60] Tao Wu, Wei-hua Zhao, Yan Dong, Hai-xin Song, and Jian-hua Li. Effectiveness of ultrasound-guided versus fluoroscopy or computed tomography scanning guidance in lumbar facet joint injections in adults with facet joint syndrome: a meta-analysis of controlled trials. *Archives of physical medicine and rehabilitation*, 97(9):1558–1563, 2016.

[61] Ling Ye, Chuanbing Wen, and Hui Liu. Ultrasound-guided versus low dose computed tomography scanning guidance for lumbar facet joint injections: same accuracy and efficiency. *BMC anesthesiology*, 18(1):160, 2018.

Curriculum Vitae

Education

The University of Western Ontario   *September 2018 - August 2020*
M.E.Sc in Biomedical Engineering, Imaging
Supervisors: Dr. Terry Peters, Dr. Elvis Chen

The University of Western Ontario   *September 2013 - April 2018*
Bachelor of Science, Specialization in Computer Science
Minor in Software Engineering

Posters and Presentations

Society of Photographic Instrumentation Engineers   *February 2020*
Oral Presentation   *Houston, Texas, US*
D. Allen, *J. Moore, C. Clarke, T. Peters, E. Chen*
Miniature C-Arm Simulator Using Wireless Accelerometer Based Tracking

Image Processing Computer Assisted Interventions   June 2019
Oral and Poster Presentation   Rennes, France
D. Allen, J. Moore, C. Clarke, T. Peters, E. Chen
Miniature C-Arm Simulator Using Wireless Accelerometer Based Tracking

Imaging Network of Ontario   *March 2019*
Oral and Poster Presentation   *London, Ontario*
D. Allen, *J. Moore, C. Clarke, T. Peters, E. Chen*
Miniature C-Arm Simulator Using Wireless Accelerometer Based Tracking

Work Experience

The University of Western Ontario   January - April (2019 and 2020)
Teaching Assistant
*TA for ES1036: Programming Fundamentals for Engineers. Responsible for running weekly
tutorials and lab sessions for first-year undergraduate students as well as marking assignments*

and exams.

Robarts Research Institute June - August 2018

Research Assistant

Worked on the software implementation of a miniature C-Arm simulator built in C++ and VTK. Responsible for the integration of the software with the hardware components.

Diebold-Nixdorf June 2016 - August 2017

Software Engineering Co-op

Worked on a team of 15 developers (including off-shore in India and Scotland) to develop and maintain an enterprise-level Automated Teller System. Responsible for finding and fixing defects and developing new features. Played a large role in designing and developing the automated test solution.

Bit by Bit Computer Camp June 2015 - August 2015

Counsellor

Taught groups the fundamentals of programming using Scratch and Python. Introduced kids to the concepts of Engineering and Design by building and programming robots. Responsible for creating a fun learning environment while ensuring that the kids obtained a firm grasp on the core concepts of logic and programming.

Volunteer Experience

Canadian Hall of Fame Workshops 2018 - Present

Student Volunteer

Ran Augmented and Virtual Reality demonstration stations for middle school and high school kids.

London Health Sciences Centre August 2018 - October 2018

Student Volunteer

Observed various spinal injection procedures under the guidance of a mobile C-Arm. Received hands-on education of the role C-Arms play in minimally-invasive interventional spine procedures.

Technical Strengths

Tools	3DSlicer, Unity, Visual Studio, QTCreator, Gimp, Eclipse, MS Office
Languages	C, C++, C#, CMake, VTK, Qt, Python, Matlab, Java, Javascript

Extra-Curricular

The University of Western Ontario   November 2019 - Present
Member
Member of the Western Squash Club.

The University of Western Ontario   January 2016 - April 2016
Team Captain
Captained a competitive Co-ed intramural ball hockey team.

Tecumseh Tennis Club   September 2016 and 2018
Member
Doubles Champions in 2016 and 2018 for the annual tournament.

Lorne Park Secondary School   June 2010
OFSAA Rugby champions
Ontario Federation of School Athletic Associations Champions.